Published in final edited form as:
J Neurophysiol. 2007 January ; 97(1): 387–406. doi:10.1152/jn.00558.2006.

Neurophysiology of Prehension. I. Posterior Parietal Cortex and Object-Oriented Hand Behaviors

Esther P. Gardner, **K. Srinivasa Babu**, **Shari D. Reitzen**, **Soumya Ghosh**, **Alice S. Brown**, **Jessie Chen**, **Anastasia L. Hall**, **Michael D. Herzlinger**, **Jane B. Kohlenstein**, and **Jin Y. Ro**
Department of Physiology and Neuroscience, New York University School of Medicine, New York, New York

Abstract

Hand manipulation neurons in areas 5 and 7b/anterior intraparietal area (AIP) of posterior parietal cortex were analyzed in three macaque monkeys during a trained prehension task. Digital video recordings of hand kinematics synchronized to neuronal spike trains were used to correlate firing rates of 128 neurons with hand actions as the animals grasped and lifted rectangular and round objects. We distinguished seven task stages: approach, contact, grasp, lift, hold, lower, and relax. Posterior parietal cortex (PPC) firing rates were highest during object acquisition; 88% of task-related area 5 neurons and 77% in AIP/7b fired maximally during stages 1, 2, or 3. Firing rates rose 200–500 ms before contact, peaked at contact, and declined after grasp was secured. 83% of area 5 neurons and 72% in AIP/7b showed significant increases in mean rates during approach as the fingers were preshaped for grasp. Somatosensory signals at contact provided feedback concerning the accuracy of reach and helped guide the hand to grasp sites. In error trials, tactile information was used to abort grasp, or to initiate corrective actions to achieve task goals. Firing rates declined as lift began. 41% of area 5 neurons and 38% in AIP/7b were inhibited during holding, and returned to baseline when grasp was relaxed. Anatomical connections suggest that area 5 provides somesthetic information to circuits linking AIP/7b to frontal motor areas involved in grasping. Area 5 may also participate in sensorimotor transformations coordinating reach and grasp behaviors and provide on-line feedback needed for goal-directed hand movements.

INTRODUCTION

Prehension is an object-oriented behavior that underlies many skilled actions of the hand. It comprises four major components: reach, grasp, manipulation, and release that appear to be mediated by different areas of the cerebral cortex, and monitored by various sensory modalities. Visual information about an object's intrinsic properties—size, shape, and identity—and its spatial location in the workspace aids motor planning of grasping (reviewed in Fogassi and Luppino 2005; Jeannerod et al. 1995; Milner and Goodale 1995; Paulignan and Jeannerod 1996; Sakata et al. 1997). The initial view of the object strongly influences the kinematics of acquisition by determining the opening of the fingers during reach as the hand is preshaped for grasp, selection of contact points on the object to promote grasp stability and efficient manipulation, and the initial rate and magnitude of grip and load forces applied by the hand

Address for reprint requests and other correspondence: E. P. Gardner, Dept. of Physiology and Neuroscience. New York University School of Medicine. 550 First Ave., MSB 442, New York, NY 10016 (gardne01@endeavor.med.nyu.edu).
Present addresses: Dr. K. Srinivasa Babu, Dept. of Neurological Sciences, Christian Medical College, Vellore – 632 004, India; S. Ghosh, Centre for Neuromuscular and Neurological Disorders, University of Western Australia, Queen Elizabeth II Medical Centre. Nedlands, Perth, Western Australia 6009; S. D. Reitzen, Dept. of Otolaryngology, New York University Medical Center, 550 First Ave., New York, NY 10016; J. Y. Ro, Dept. of Biomedical Sciences, Program in Neuroscience, University of Maryland Dental School, 666 W. Baltimore St., Room 5C-06, Baltimore, MD 21201.

on contact. Hand preshaping to object size and shape during reach is characteristic of normal primate hand function (Chieffi and Gentilucci 1993; Jeannerod 1986, 1994; Jeannerod et al. 1995; Roy et al. 2000, 2002) and is disrupted by lesions of anterior zones of posterior parietal cortex (PPC) in humans and monkeys (Gallese et al. 1994; Goodale and Westwood 2004; Jeannerod et al. 1994, 1995; LaMotte and Acuña 1978; Milner and Goodale 1995; Pause and Freund 1989; Pause et al. 1989; Tunik et al. 2005) and their projection sites in the frontal lobe (Fogassi et al. 2001).

PPC is thought to be an important nexus in motor planning of prehension because its anatomical connections with both the dorsal stream of vision and the somatosensory areas of the anterior parietal lobe allow it to combine visual and postural information to develop a plan of action. Since the early studies of Mountcastle et al. (1975), it is well established that neurons in PPC play a significant role in reaching, pointing and grasping behaviors (reviewed in Andersen and Buneo 2002; Andersen et al. 1997; Battaglia-Mayer et al. 2003; Caminiti et al. 1998; Fogassi and Luppino 2005; Hyvärinen 1981; Jeannerod et al. 1995; Kalaska 1996; Kalaska et al. 1997; Wise et al. 1997). Collectively, these studies implicate PPC in sensorimotor transformations needed to direct the hand to objects of behavioral interest such as food and to acquire them for consumption.

Single-cell recordings in monkeys and functional imaging of human cerebral cortex indicate that reach and grasp are temporally synchronized but controlled by distinct networks of neurons in parietal cortex (Binkowski et al. 1998Binkowski et al. 1999; Chieffi and Gentilucci 1993; Culham et al. 2003; Ehrsson et al. 2000; Frey et al. 2005; Grafton et al. 1996; Shikata et al. 2003; Tunik et al. 2005). Anatomical segregation of neurons tuned to reach and grasp behaviors was first reported by Mountcastle and co-workers (1975), who noted that hand-manipulation neurons in both area 5 and area 7 were more likely to be recorded on electrode tracks placed more laterally than those in which arm projection neurons were encountered. Subsequent investigations confirmed and extended these findings. Sakata and coworkers (Murata et al. 1996, 2000; Sakata et al. 1995, 1997, 1999; Taira et al. 1990) and Fogassi and Luppino (2005) demonstrated that neurons in the anterior intraparietal area (AIP) of the inferior parietal lobule responded to viewing objects as well as grasping them in trained tasks. Clear synergies occurred between observation and action in their task, and many of the cells responded preferentially to grasp and/or view of particular objects. They proposed that firing rates of AIP neurons might be used to select the appropriate grasp posture needed to acquire objects of specific sizes or shapes.

Hand manipulation neurons in area 5 were not studied after the original description by Mountcastle and co-workers (1975) until our laboratory adapted digital video to quantify hand behaviors during prehension (Debowy et al. 2001; Gardner et al. 1999, 2002; Ro et al. 1998, 2000). Using a grasp-and-lift task to compare firing patterns in primary somatosensory (S-I) cortex and PPC, we found that the onset of activity in PPC preceded that in S-I. This was a somewhat surprising finding to us, because the anatomical connectivity between S-I and PPC suggested that areas 5 and 7b occupied higher levels in the hierarchical organization of somatosensory areas of the cerebral cortex (reviewed in Felleman and Van Essen 1991). Furthermore, neurons in the rostral bank of the intraparietal sulcus (IPS) hand representation were shown to have more complex physiological responses to somatosensory stimuli than those of neurons in areas 3b, 1, and 2 (Darian-Smith et al. 1984; Duffy and Burchfield 1971; Iwamura and Tanaka 1978; Iwamura et al. 1993, 1995; Sakata et al. 1973).

In this report, we extended our original studies of prehension to additional animals to compare responses in the hand representation of area 5 to neurons in area AIP and the adjacent inferior parietal lobule (area 7b or PF/PFG). Each of the three monkeys studied used an individualized hand posture to grasp the objects, allowing us to determine whether the firing patterns observed

in our initial studies could be generalized to the various muscle synergies used by each subject. The data presented in this report confirm and extend our earlier studies, indicating that neurons in both subregions of PPC serve a sensorimotor function during acquisition of objects by the hand. These neurons also receive somatosensory feedback that appears to confirm the expectations of reach and grasp actions, and enable corrective maneuvers of the hand if the desired action was unsuccessful.

METHODS

Neurophysiological and behavioral data were obtained from three adult rhesus monkeys (*Macaca mulatta*, 2 male and 1 female, weight: 8–16 kg), trained to perform a prehension task. Experimental protocols used in this study were reviewed and approved by the New York University Medical Center Institutional Animal Care and Use Committee (IACUC) and are in accordance with the guiding principles for the care and use of experimental animals approved by the Councils of the American Physiological Society, the National Research Council, and the Society for Neuroscience.

Prehension task

The prehension task required the animals to grasp and lift objects using visual cues displayed on a computer monitor to select the appropriate one. The test objects were a set of four knobs mounted on a box placed at arm's length, 22–24 cm in front of the animal (Fig. 1). When testing the right arm, the knobs were arrayed left to right (1) in front of the monkey's left shoulder, (2) at the midline, (3) in front of the right shoulder, and (4) lateral to the right shoulder. The shape box was shifted to the left in recording sessions from the right hemisphere when testing the left arm. The knob shapes tested included rectangular blocks (20 × 20 × 40 mm), large and small round knobs (30 or 15 mm diam), and a cylinder (40 × 15 mm diam). The total load was adjusted with weights inside the shape box and ranged were 108 g (small round), 137 g (rectangle), 140 g (cylinder), and 242 g (large round). The knobs were lifted using a whole-hand power grasp between fingers and palm. The animals could view the workspace, including all four knobs, and used visual guidance to position the hand on the objects. Some neurons were also tested with view of the shape box and hands blocked by an opaque plate inserted in the chair frame below the chin.

The knob to be lifted was cued in blocks of 2–10 trials by a Commodore 64 computer. The locations of the four knobs in the workspace were represented on a color monitor by four identical black icons; one icon was flashed in red to indicate which knob should be lifted. As lift began, the icon at the corresponding location moved upward on the screen to reinforce the desired behavior and changed color at the top position. If the correct knob was selected, the icon turned white, and the monkey received 0.1 ml of dilute infant fruit puree (applesauce or bananas). If an incorrect knob was lifted, the icon turned cyan and there was no reward. The icon color reverted to black when the knob was returned to the rest position. Cues for the next trial appeared after a 1.5-s delay interval in studies of *monkeys H17094* and *N18588;* cues were presented immediately after the knob was replaced on the box in experiments with *monkey B2195*.

Trials were self-paced, without external time constraints on trial initiation or duration. Task performance mimicked natural grasping behaviors in that the animals were allowed almost complete freedom of execution so long as they fulfilled the basic goals of acquiring and lifting the designated object. The monkey could freely choose how to position its hand on the knob so long as the grasp posture secured it during lifting. Animals were not required to remove the hand from the workspace between trials and often left part of the hand touching the knob in anticipation of possible repeats of the same cue.

Digital video monitoring of hand kinematics

The monkey's hand movements were monitored by sets of digital video (DV) cameras at 29.97 frame/s and digitized in the camera itself (Canon XL-1 and Sony TRV900 Mini-DV camcorders) or with a digitizer board (Radius Video Vision Studio and Sony CCD-VX3 color Hi-8 camcorders). This system provided synchronized digitized records of neuronal spike trains that were correlated directly to matching video images using frame time codes (Debowy et al. 2002; Ro et al. 1998). The DV format provided high-definition image quality using consumer-grade, inexpensive DV camcorders that compressed 720 × 480 pixel video images to 3.1 MB with MPEG-2 sampling; spike trains were recorded and digitized at the same time on the camcorder's audio channels. Camcorders provided lateral, frontal, and/or overhead real-time views of the monkey and the workspace, and stored kinematic records of the animal's behavior on videotapes; simultaneously acquired neuronal responses, fed from the electrophysiological amplifiers, were recorded on the audio track.

Digital editing software (Final Cut Pro version 3 or Adobe Premiere version 5.1) was used to download clips of the experiment via the Firewire ports of Macintosh G4 or IMac computers and stored as QuickTime movie files. Hand behaviors were viewed in real time, at high speed, or in frame-by-frame mode. Forward and backward bracketing of sequential frames was particularly useful for visualizing how the hand posture changed over time and for compiling event logs of the start times of the task stages on each trial. These event time codes were stored in spreadsheets and were used subsequently by the software tools as markers for alignment of neural responses in rasters and peristimulus time histograms (PSTHs) and for bracketing task stages in statistical analyses of firing rates.

To further delinate the trajectory of hand movements during the task, we exported sets of sequential video frames as TIFF files that were placed in separate layers of Adobe Illustrator files. The pen tool was used to trace outlines of the monkey's arm, hand, and fingers in each frame, as well as the shape box and knobs, to construct a time series of kinematic drawings (Reitzen et al. 2004). Successive frames were aligned in separate layers and overlapped as shown in Fig. 1. The topmost drawings were made transparent, allowing the underlying layers to be visualized. In this way, the trajectory used by the hand to acquire and manipulate objects, and the dynamics of movement could be viewed directly in single images.

The kinematic drawings also provided an objective standard for parsing hand movements into seven distinct stages plus an intertrial interval (stage 0). Actions subsumed in each stage are illustrated in the hand tracings of Fig. 1. 1) *Approach*: the reach interval, which began as the animal projected the hand toward an object (red), and ended when the hand contacted it (yellow). The hand was preshaped during approach, assuming a posture that anticipated object acquisition. *2*) *Contact*: the hand positioning interval that spanned the period between initial touch (yellow) and full enclosure of the knob between the fingers and palm as it was grasped (orange). *3*) *Grasp*: static enclosure of the knob in the hand prior to lift. Although the knob was sometimes rotated during the grasp stage, there was no further tangential motion of the hand over its surface. *4*) *Lift*: upward displacement of the knob from rest (light blue) to the top position (magenta). *5*) *Hold*: maintained elevation of the knob at the upper stop. *6*) *Lower*: downward replacement of the knob through relaxation of grasp (cyan). *7*) *Relax*: maintained hand contact on the knob in a relaxed posture.

The relax stage was succeeded by regrasp of the test object or by hand withdrawal from the knob. Release of a knob was followed by lateral reach to a new knob, initiating another trial, or removal of the hand from the workspace.

Stages 1–3 were required for object acquisition, stages 4 and 5 for manipulation, and stages 6–7 for release of the object. The time codes of these events were logged from the single frame views, and used as event markers for spike data analysis.

Surgical and recording techniques

Extracellular single-unit recordings were made in the left hemisphere of *B2195* and *H17094*, and in both the left and right hemispheres of the third animal (*N18588*) as they performed the prehension task. Using techniques for chronic single-unit recordings developed by Gardner and Costanzo (1980) and Warren et al. (1986), a stainless steel chamber was permanently implanted over the postcentral gyrus hand area in an aseptic surgical procedure under general anesthesia (1.5–3% isoflurane mixed with 2–3 l/min of O_2). The dura was left intact to prevent infection and contain brain swelling. The recording chamber provided access to a 25-mm-diam region of cortex centered 2–4 mm posterior, and 18–20 mm lateral to the bregma; the rostral end was situated 2–5 mm anterior to the central sulcus, and the caudal end was located over the inferior parietal lobule. The chamber was sealed with a transparent Lucite cap, except during recording sessions when the cap was replaced with a sterile Silastic membrane held in a stainless steel ring. A pair of stainless steel screws (size 6–32) cemented to the occipital skull limited head movements during recording sessions to small vertical displacements to maximize the stability of spike train recordings.

Buprenex (buprenorphine hydrochloride, 0.01 mg/kg bid) was administered for a 4-day period after the surgery to alleviate postoperative pain. Solu-Medrol (methylprednisolone sodium succinate; 5 mg/kg im) was given immediately after surgery, and on the following day, to reduce brain swelling. Intraoperative antibiotics [Baytril (enrofloxacin) solution; 1 mg/kg] were supplemented with once-daily doses for 6 –7 days postoperatively. The interior of the chamber was rinsed with 35–50 ml sterile saline before and after each recording session, and the wound margins were washed with surgical sponges and hydrogen peroxide. Topical antibiotics (gentamycin or Baytril) were applied as necessary to the implant site.

Extracellular recordings of spike trains in the left hemisphere were made with epoxylite-insulated tungsten microelectrodes (FHC, Model UEWLFELE2N1X, impedance = 2 MΩ) advanced through the intact dura and into the brain by a remotely operated miniature stepping hydraulic motor (David Kopf Instruments, Model No. 607W). Microelectrode recordings in the right hemisphere of *N18588* used a computer-controlled multiple electrode positioning system (Alpha Omega EPS-MT) that allowed simultaneous recordings from four independently mobile tungsten microelectrodes. Recording depth was calibrated from the microdrive reading; the depth at which the electrode exited the cortex at the end of the session was subtracted from that of the recording site to yield its approximate intracortical location.

Calibrated positioning guides placed within the chamber lumen specified the actual site of microelectrode insertion. In single-electrode studies, different combinations of two guides allowed us to establish a recording site's radial distance from the center of the chamber and angular displacement from the midline with 0.25 mm precision. The position of the multielectrode guide tube was indicated on a vernier in anterior-posterior and medial-lateral coordinates relative to the chamber center, accurate to 0.1 mm. The position of each penetration site was marked on photographs of the brain made during surgery, creating a functional micromap.

Spike trains were amplified and filtered (band-pass 100 Hz to 3 kHz, Grass P511 amplifiers or Cyberamps, Axon Instruments), displayed on oscilloscopes and/or computer monitors, and digitized at 16-bit resolution, 48 kHz, or 12-bit resolution, 32 kHz, by the DV camcorders. The same spike data were captured on all three cameras, allowing precise synchronization of their audio and video tracks. The digitized spike trains were downloaded to the lab computers

together with the video clips of the animal's behavior and stored as both QuickTime audio signals and in Audio Interchange file format (AIFF) for quantitative analyses of firing patterns. The raw spike trains were displayed by the editing software as a strip chart in a separate window for the audio waveform, allowing us to correlate hand movements shown in the video window with the corresponding portion of the spike train. As video and spike trains were recorded and digitized simultaneously, both datasets spanned the same time interval. Hence, knowledge of the time code of each video frame in the clip provided a precise way to locate the matching firing patterns. Similarly, measurements of the timing of spikes with respect to the onset of the audio data sample placed each spike in a precisely designated video frame.

Firing patterns of cortical neurons were analyzed directly from the AIFF files using interactive clustering to distinguish neuronal action potentials from noise and to separate the spike waveforms of up to four different neurons recorded from each electrode into individual traces (Ro et al. 1998; Sherwood et al. 2006). A list of consecutive spike time stamps was obtained for each neuron to construct continuous displays of firing rates and perform other analyses. Neurons had to be recorded for ≥5 min to capture a sufficient number of task trials for statistical analyses.

Quantitative analyses of neuronal responses

Burst analysis graphs (Fig. 2) providing a continuous record of neural and behavioral events within a video clip were used to screen neural responses to the task. Burst analysis provided an objective mechanism for correlating periods of high neuronal firing with behavioral activity as it relied on the responses of the neuron as an alignment metric rather than subjective standardization of the animal's actions. Spike trains were represented as rasters and continuous binned firing rates together with markers of actions performed by the monkey and/or experimenter during the clip. Reverse correlation of periods of high firing (green "burst" trace) with the matching video images of the monkey's behavior at the burst start, peak, and end times were used to highlight the behaviors to which a neuron was most responsive. We chose 100 ms as the minimum burst duration because it spanned three complete video frames in NTSC format and 2.5 frames in PAL (30 and 25 fps US and European video standards). The burst threshold was set one SD above the mean rate per 100-ms bin compiled during the entire 2- to 3-min clip. This protocol allowed us to determine whether we could predict what the animal was doing by simply examining continuous spike train data. By repeating the process of frame captures for the largest bursts, we examined whether there was a reliable relationship between neuronal activity and the kinematics of prehension. The linkage between bursts and task kinematics suggested the most relevant task stage(s) on which to trigger PSTHs and rasters. Neurons without a clear response to the trained task or to spontaneous grasp behaviors were not subjected to further analyses.

Spike rasters and PSTHs were aligned to the frame onset times of specific task behaviors such as hand contact with the knob. Data from individual trials were binned with 10-ms resolution and grouped in spreadsheets to construct PSTHs for specific knobs, grasp styles, behavioral conditions, or video clips. The time base of PSTHs and rasters was scaled to the duration of each monkey's task performance to include data from all stages of the task plus a generous portion of the intertrial interval.

Further quantification of task-related activity was obtained from measurements of *mean firing rates per stage* on each trial. Responses on all trials were averaged to compile firing rate profiles for each neuron during the pretrial interval and the individual task stages. Neuronal activity during successive actions was more accurately depicted by average firing rate graphs because the PSTH profile was somewhat dependent on the event selected to align spike trains and variable task stage duration across trials. Neurons were grouped by the stage(s) that evoked

maximum firing and subdivided into classes tuned to single actions, two successive actions, or broadly tuned classes by statistical comparison of mean rates during sequential task stages.

The individual trial data were used for statistical analyses and to further classify responses. A repeated-measures ANOVA model (Stat-View, SAS Institute) analyzed whether each neuron demonstrated significant modulation of firing rates across the seven task stages and the pretrial interval (F-test, $P < 0.05$). Firing rates between stage markers on each trial were within-subject variables and the task conditions (knob grasped, approach style, hand used) between-subject variables. Nearly all of the task-related neurons yielded $P < 0.001$ on F-tests. In addition, task-related neurons were required to show significantly increased or decreased firing rates during at least one task stage compared with the pretrial rate in paired means comparisons ($P < 0.05$).

Histological localization of recording sites

Both physiological and neuroanatomical techniques were used to locate recording sites. As the monkeys were studied for periods of ≤ 2 yr, it was not possible to recover the precise electrode tracks for all but the last few in any brain. Instead we used the putative entry points of the microelectrodes into the cortex to localize the recording sites. These methods allowed us to reconstruct the antero-posterior (A-P) and medio-lateral (M-L) coordinates of electrode tracks; recording site depth along the track was approximate. Small errors in track localization were inevitable, especially at borders between areas. However, physiological properties of neurons recorded along the electrode tracks were consistent with the stated designations.

In selected sessions, we used electrodes coated with DiI or DiI-5 to mark recording sites of particular interest following protocols of DiCarlo et al. (1996). In addition, 16 –20 days before death, injections of fluorescent dyes (fast blue, diamidino yellow, fluororuby) and dextran-conjugated tracers (dextran alexa, dextran biotin) were made in two of the three animals at sites that had yielded particularly interesting data on earlier penetrations to help localize those tracks in the cortex. Injection sites were also marked with microelectrodes dipped in DiO and inserted manually through the micropositioner. This left a blue trace that was visible during cryosectioning of the brain, helping to localize dye injections to particular histological sections.

The animals were killed by an overdose of intravenous barbiturate anesthetic (Nembutal, 120 mg/kg) following the current guidelines established by the American Veterinary Medical Association. The brain was prepared for histology by intracardiac perfusion with saline, followed by 4 l of 10% buffered formalin. The A-P and M-L boundaries of the recording chamber were marked using stainless steel hypodermic tubing (24 gauge) dipped in India ink or electrodes coated in DiO inserted through the micropositioner. The brain was photographed, and the reference marks used to align the map of recording sites on the cortical surface. Frozen histological sections were cut in the coronal or horizontal planes and stained with cresyl violet, or prepared for fluorescence microscopy.

Recording sites were reconstructed from serial sections. Histologically identified tracer injection sites were used to align the entry sites into the cortex and to extrapolate the locations of other recording tracks. The postcentral gyrus hand area was divided into three cytoarchitectural zones based on criteria set forth by Pons et al. (1985) and Lewis et al. (Lewis and Van Essen 2000a,b; Lewis et al. 1999). Area 3b-1, the most anterior zone of S-I cortex, included penetrations within a band 2 mm caudal to the central sulcus. Posterior S-I comprised the next 3– 4 mm on the exposed gyrus, and was denoted as area 2. PPC comprised cortical areas surrounding the IPS and was divided into superior and inferior parietal lobules. The superior parietal lobule (SPL) included the rostral bank between area 2 and fundus of the IPS, corresponding to Brodmann's area 5. Neurons recorded in the exposed bank of the SPL were labeled area 5d following the terminology of Lewis and Van Essen (2000a), whereas those in the rostral bank of the IPS were labeled area 5v. Similarly, IPL neurons recorded in the caudal

bank of the IPS near its anterior end were designated as in area AIP (Murata et al. 2000), whereas those in the adjacent lateral convexity of the IPL were designated as in area 7b (Cavada and Goldman-Rakic 1989a; Lewis and Van Essen 2000a); the latter region includes areas PF and PFG of Pandya and Selzer (1982).

RESULTS

Cortical recordings were made with the intent to maximize the number of neurons the firing patterns of which could be linked reliably to the actions of the hand during the prehension task. Tracks (294) were made in the cortices of the three animals as indicated in Fig. 3. The widest sampling of cortical areas was made in *monkey B2195*; recording sites in *monkeys H17094* and *N18588* were concentrated in posterior parietal cortex around the lateral IPS and in posterior S-I. This report describes neuronal firing patterns of 85 neurons in area 5d/5v and 43 cells recorded in area AIP/7b during the task. As responses to the four test objects were similar in time course, we pooled data from trials of the round and rectangular knobs for these analyses.

Area 5 neurons respond to object acquisition

Figure 4 illustrates the kinematics of task performance captured during two successive trials for *monkey H17094.* In these examples, the trials began as the animal rested its hand on the chair frame and viewed the computer screen. The onset of reach coincided with or followed a saccade to the cued object. Approach was direct and rapid. Reaches had arc-like trajectories that spanned five to six video frames (167–200 ms) with peak velocity at the midpoint of travel. The fingers were preshaped for efficient grasp, and the hand simultaneously rotated downward so that the fingers contacted the side of the knob at the end of the reach (yellow). The animal grasped the knob in two frames (67 ms) by sliding digits 2–5 along its lateral face and pressing the base against the interdigital palm pads with the thumb on the top surface or parallel to the other fingers (orange). After rotation of the knob to a comfortable position, lift began. The knob was held above the box, as the animal consumed the juice reward and then was lowered and the grip relaxed. Note the common gestures used on the two trials.

Figure 5 shows the corresponding spike trains of a pair of simultaneously recorded area 5v neurons in burst analysis format together with temporal markers of the hand actions. Each set of upward and downward deflections in the yellow task stage trace denotes a single trial; four trials were performed during this 20-s period. The approach, contact, grasp and lift stages (1st 4 upward deflections of the yellow trace) were relatively brief and of similar time course from trial to trial, whereas later stages were prolonged and more variable in duration. Periods of high firing and co-activation of the two neurons coincided with stages 1– 4 when the object was acquired in the hand. Both neurons increased their firing at the start of approach, fired at maximum rates just prior to or at contact, and then decreased their firing rates as the object was grasped by the hand and lifted.

Reverse correlation of periods of high firing with the matching video images confirmed the neuron's sensitivity to specific actions. When the spike train was objectively parsed into periods of above and below threshold activity, all of the large bursts (green trace) occurred on acquisition of one of the knobs. The frame captures to the right correspond to the peaks of bursts A–C. Firing was maximal during the approach to the right rectangle when the hand was preshaped (bursts A and B), and at contact with the small round knob (burst C). The gaze continued to focus on the knob in burst B but had returned to the computer screen in bursts A and C.

Regrasp of the same knob without a reach and preshape stage failed to produce the same high firing rates from either neuron. During burst D, the animal relaxed the grasp but did not break contact with the rectangle knob. Instead, as diagrammed in Fig. 6, he slid digits 4 and 5 under

the knob and pushed it upward without fully grasping it. Neural responses were weaker than during bursts A–C, and only one of the two cells fired above threshold. Burst E occurred as the hand was withdrawn from the rectangle knob and projected laterally in the direction of the large round knob. However, the approach was spontaneously aborted, and the hand returned to the chair frame, which was approached and grasped in the same manner as the rectangular knobs. The neural response during burst E paralleled the kinematic sequence in the task, starting during hand withdrawal, peaking midway through reach, and ending prior to contacting the chair. Similar acquisition evoked activity was observed when the animal grasped other objects in the workspace such as food morsels (Babu et al. 2000).

Higher temporal resolution of the spike trains of these two cells is provided in Fig. 7 by rasters and PSTHs aligned to hand contact with the knobs. The neuronal firing patterns on each trial depended on the timing of prehension behaviors. High firing rates spanned the interval between the onset of approach and lift. The expanded time base demonstrates that the firing rate increased abruptly as approach began (gold marker) regardless of the knob shape or location in the workspace. The rise in firing occurred as early as 250 ms before contact (red marker) and continued at high levels until the knob was secured in the hand (magenta marker). Thus neural activity began before active tactile stimulation of the hand. The firing rate was highest at contact and decreased as grasp was secured. Firing rates dropped still further during lift (dark blue) and returned to baseline during hold (light blue). Although the object was tightly pressed against the glabrous skin of the hand during the hold stage, firing rates remained low until another trial was initiated. The response time course suggests that these neurons signaled the acquisition actions of the hand rather than direct tactile stimulation by the objects.

Strong responses to object acquisition were typical of area 5 neurons recorded in all three animals. Figure 8 displays contact-aligned rasters and PSTHs from four neurons recorded simultaneously in the right hemisphere of another monkey (*N18588*). Although this animal used a different grasp posture (Fig. 13), the phasic responses to object acquisition in Fig. 8, *A* and *B*, had similar spatiotemporal profiles to those of the neurons in Fig. 7. Their firing rates rose at or before the mean onset of approach, peaked during contact or grasp, and declined to or below baseline during the hold stage. Similar responses were reported previously from the third animal (*B2195*) when tested with just the rectangular knob (Gardner et al. 1999).

The neurons illustrated in Fig. 8, *C* and *D*, were recorded simultaneously from two additional electrodes of the multielectrode array placed 0.5 mm away. Although all four neurons fired maximally during the contact and/or grasp stage, they showed slightly different spatiotemporal profiles. Neurons recorded simultaneously on the *same* electrode generally showed similar firing patterns; cells with the smallest amplitude spikes usually displayed the highest firing rates, and earliest onset times (Figs. 7, *bottom*, and 8*A*). Neurons recorded on different electrodes showed greater diversity of firing patterns. In this grouping, the earliest task-related activity began on electrode 4 before the visible onset of reach (Fig. 8*D*). Although these responses were somewhat variable from trial to trial, the increase in firing predicted the beginning of a trial. Responses on electrode 1 began slightly later with the start of approach (Fig. 8, *A* and *B*), whereas those on electrode 2 began just prior to contact (Fig. 8*C*). Neurons recorded on a fourth electrode had only a vague association of firing patterns to the task (not shown). Although firing rates of the four cells illustrated were reduced during hold and the relaxation of grasp, only the cells on electrode 1 were inhibited during these late task stages. Relaxation of grasp was signaled by another burst of activity on electrode 4. Thus the ensemble response provided greater information about hand actions than any individual neuron.

Further quantification of task-related activity was obtained from measurements of average firing rates per stage on each trial. Sample mean firing rate graphs of hand manipulation neurons in area 5v/5d are shown in Fig. 9; the data illustrated are typical of 86% of SPL neurons and

include responses of the neurons in Figs. 7 and 8 (*J–K* and *D, H, L*, and *M*, respectively). Epochs of high firing bridged the period from approach through lift but varied in relative intensity among individual neurons. All of the cells illustrated showed a significant rise in firing rate during approach, before the hand touched the objects (stage 1, $P < 0.001$). This activity was maintained or rose in intensity on tactile stimulation of the hand at contact; 9 of the 12 cells displayed the most intense firing at contact (stage 2). Elevated firing persisted during grasp and lift stages in most of these cells, but dropped precipitously during hold (stage 5) when hand movement ceased.

The intensity and specificity of firing during successive task actions was used to classify neuronal responses. Neurons were grouped by the stage(s) that evoked maximum firing and subdivided into classes tuned to single actions, two successive actions, or broadly tuned classes by statistical comparison of mean rates during sequential task stages. The distribution of response classes in the population studied is listed in Table 1. The most common type was broadly tuned, comprising 38% of the population. These neurons showed strong excitation during the task compared with baseline, but little distinction in firing rates between three or more successive actions in the preferred stages (Type BT, Fig. 9, *A–D*). 48% of neurons showed tuned activity focused on stages 1 and/or 2. The most commonly observed class was called contact-tuned (Type 2, Fig. 9, *J–L*) because its members fired at significantly higher rates during stage 2 than in the preceding approach stage or the following grasp stage ($P < 0.05$). PSTHs of contact-tuned neurons peaked midway through stage 2 (Fig. 7, 8A). Similarly, approach-tuned neurons (Type 1, Fig. 9, *E* and *F*) fired at higher rates during approach than in any other task stage; their PSTHs peaked before contact. Other area 5 neurons fired intensely during two successive stages, and were classified as approach-contact (Type 1.5, Fig. 9, *G* and *H*) or contact-grasp (Type 2.5, Fig. 9*M*). Mean firing rates did not differ significantly during these actions ($P > 0.05$), and their PSTHs peaked at the moment of contact (Fig. 8*B*) or grasp (Fig. 8*C*). Note that firing rates of the tuned neurons and dual-action cells were often significantly higher than baseline during other stages ($P < 0.05$) but failed to match the rates evoked during the preferred actions.

Area AIP/7b neurons also signal object acquisition

Responses to prehension in the adjacent hand representation of the IPL were similar to those recorded in area 5 of the SPL. As previously noted by Sakata and co-workers using a different grasp task, firing patterns of areas AIP and 7b neurons appeared to reflect the preparation and execution of grasping behaviors. We found that reaching, touching and grasping evoked stronger neuronal responses in IPL neurons than lifting, holding, and lowering the knobs. Each component stage of the task contributed to the evoked activity, as can be seen most clearly in burst analysis graphs.

Figure 10 illustrates 16 s of continuous recordings from an area AIP neuron in *monkey B2195* as she alternated between task performance and other spontaneous hand actions. When not engaged in the task, the neuron was silent (red *A, B, C*). It fired strong bursts at rates > 100 spikes/s on initiation of a task trial, particularly when the animal reached toward a knob from outside the immediate work-space of the shape box (blue A, G, H). The burst amplitude was high regardless of whether the hand started to reach from below (blue A) or above the knobs (blue G, H). Firing rates were independent of the shape of the target object. The bursts peaked as the hand was preshaped to grasp both round (blue A, G) and rectangular knobs (blue H) and ended when the hand touched and grasped them. Responses were stronger when the hand was properly aimed to the knob and grasp was completed (blue A, G) than when the hand fell between knobs and failed to secure one of them (blue H). In the latter case, the firing rate dropped abruptly, and the animal made a corrective lateral reach to the intended object accompanied by a second burst of impulses (blue I).

Lateral reaches between knobs evoked weaker bursts that began as grasp of one knob was relaxed, peaked during hand preshaping, and ended as the next object was contacted (blue B, I). Regrasp trials in which the animal did not relax the grasp evoked modest responses (blue C) as they lacked an approach or preshaping component, but trials in which the knob was released from grasp and the hand preshaped prior to regrasp on the next trial were quite strong (blue D, E).

The neuron was much less active when the animal engaged in behaviors other than object acquisition. Figure 11 shows actions that occurred during periods when the neuron was silent or fired sporadically. These included resting the hand on the base of the shape box (A), striking the base plate with the fist (*E*), or lifting the hand toward the face for inspection or grooming (*B, C, D,* and *F*). The neuron was sensitive to specific flexed hand postures only if they were used in the context of object acquisition. Indeed, even when the hand posture resembled that observed during preshaping (Fig. 11, *B* and *C*) or static grasp (*D–F*), the neuron remained silent if the goal of the action was something other than grasping objects. In this manner, the neuron signaled the coincidence of specific tactile and proprioceptive inputs with particular intentions.

Sensitivity to multiple task stages was also observed in the other two animals studied. Typical PSTHs and average firing rate graphs of area AIP neurons are shown in Fig. 12; similar responses were recorded in area 7b. AIP spike trains tended to last longer than those in area 5, and the task stages were less clearly distinguished. Task related activity typically began during stage 1, persisted through stage 3, when the object was fully secured in the grasp, and into stage 4 as the knob was lifted. Consequently, broadly-tuned neurons (Type BT) were the most common type observed in the population, comprising 51% of IPL neurons analyzed (Table 1). The broad sensitivity of these neurons to multiple task stages suggested that they participated in both the planning and execution of acquisition behaviors. Although the percentage of contact-tuned responses was similar to that observed in area 5, the other tuned and dual-action classes were less densely represented. In addition, 11% of IPL neurons were classified as grasp-inhibited (Type GI), because their activity was suppressed below baseline during task performance.

PPC responses are linked to motor schemas for grasping not hand postures

Although each animal developed personalized strategies and postures for grasping these objects, the hand kinematics of each one remained consistent both within a session and over the period of study. Our digital video methods allowed us to assess the detailed kinematics of prehension on a trial-by-trial basis. Images in Fig. 13, *A* and *B*, show the grasp postures used by *monkey H17094* during three sequential trials recorded on tracks 10 and 110 spaced 6 mo apart. He grasped all of the knobs with similar postures, placing the hand on their lateral aspect with the radial surface upward. The round knobs were clasped tightly between the digits and palm along their lateral sides in a whole hand power grasp, but greater flexion occurred in trials testing the small round knob. The postures were nearly identical to those shown in Figs. 1 and 5 from track 131.

Monkey N18588 used a different hand posture to grasp the knobs, scooping them upward from below with the hand supinated or holding their shaft while pushing them upward (Fig. 13, *C* and *D*). He was somewhat clumsier than the other two animals, particularly when using his left hand, and showed greater variety in hand postures from trial to trial. Some of the intertrial variability may be related to the lack of visual guidance of his actions, as he rarely looked at the knobs before acquisition but instead focused on the computer monitor for cues or stared at other irrelevant targets.

Monkey B2195 used yet another grasp strategy. She aimed her hand toward the top surface of the knobs, made contact on the glabrous surface of the proximal phalanges, rather than on the

digit tips, and used the heel of the palm to push the knobs upward (Fig. 10). As previously documented (Ro et al. 1998;Gardner et al. 1999), she used this overhand grasp posture throughout the 1-yr period of study.

Despite the different grasp styles used by these animals, the stage timing was roughly the same for all three monkeys (Table 2). Their task behavior remained within a narrow range from session to session; trial duration (approach through relax) ranged from 1.02 to 1.92 s in the three animals. The least variability in performance time occurred during acquisition stages that were crucial for reward. Static grasp was the shortest stage, spanning one to four frames as the animals transitioned rapidly from grasp to lift in this highly practiced behavior. Later stages were more variable in duration, from trial to trial and between individual monkeys because the principal action was consumption of the juice reward. Grasp usually was not released until licking ended.

The neural responses we recorded seemed to be correlated primarily with actions of the hand rather than visual stimulation by the objects. Unlike earlier studies of area AIP, all of the test objects were visible to the animal throughout the session. Although neural activity at the onset of reach often coincided with gaze fixation on the object, these putative visual responses occurred only in the context of an impending or on-going acquisition behavior, and usually outlasted the period of gaze (see e.g., gaze trace, Fig. 5). Furthermore, although grasping movements were more precise when the animal looked at the object, preliminary data suggest that there was little difference in average firing rates during the task when view of the workspace and hands was blocked by an opaque plate placed below the animal's chin.

Population responses to prehension in PPC

The consistent kinematic behaviors of each animal allowed us to compare neuronal behaviors between animals and across cortical areas over the period of study, and thereby measure population responses. Average firing rate graphs were used to quantify the distribution of preferred actions in the population of 128 hand manipulation neurons studied. Contact and hand positioning on the knob during stage 2 was the most strongly represented action in both the SPL and IPL populations (Fig. 14). 44% of area 5 neurons (37/85), and 28% of area AIP/7b neurons (12/43), fired maximally during stage 2. Another 28% of area 5 neurons (24/85), and 23% of AIP/7b cells (10/43), fired at highest rates during approach before the hand touched the knobs. In this manner, firing patterns correlated to the initial acquisition of objects were most salient in area 5, where 72% (61/85) of neurons fired at their highest rates during stages 1 and 2, and in AIP/7b, where 51% fired maximally. Static grasp was less effective than touching, particularly in area 5, where 16% of cells fired at peak rates in stage 3; more than half of these neurons were broadly tuned, meaning that their firing rates during contact and/or lift stages were not significantly lower. Similarly, while a higher percentage of AIP/7b neurons had peak activity during grasp (26%), nearly all of these cells were broadly tuned. Only 7% of hand manipulation neurons fired maximally during lift, but with only one exception, all were classified as broadly tuned. Holding was the least effective action; only 1 of 128 neurons responded maximally in stage 5.

The focus of PPC activity on acquisition behaviors was also observed in the mean population firing rates. We normalized each neuron's response profile as a function of the firing rate during the peak stage to calculate the population average response (Fig. 15). Firing rates in both regions of PPC were significantly higher than baseline during stages 1– 4 (approach through lift) and fell below baseline during the remainder of the task. Hand manipulation neurons in area 5 fired at highest rates during approach and at contact, whereas static grasping and lift evoked progressively weaker responses. Maintained grasp in the hold stage inhibited area 5 responses, suggesting that tactile information from the hand was suppressed once the task goals had been

accomplished. Averaged activity in area AIP/7b was similar to that recorded in area 5, but grasp responses were slightly stronger, and inhibition less prevalent in the later task stages.

Finally, we examined the extent of representation of particular hand actions in the two populations. We used paired means tests to compare average firing rates during each task stage to the pretrial mean rate to determine the relative proportion of neurons that were significantly excited or inhibited by each action. Statistically significant increases in firing rates occurred in both SPL and IPL neurons during stages 1– 4 (Fig. 16). The proportion of excited neurons was highest during approach and at contact (83% of area 5 neurons and 72% in AIP/7b) and fell to ~60% during lift. In later stages, significant excitation was observed in < 5% of SPL neurons and in 25% of IPL cells indicating that task-related excitation persisted longer in the inferior parietal lobule. Inhibition in the population increased steadily following grasp, ranging from 17% during lift to ≥40% as the knob was lowered and the grip relaxed. Depression of firing below baseline was more prevalent in area 5 than in AIP/7b.

In summary, hand manipulation neurons in both SPL and IPL were found to be active during the planning of grasp as the hand was preshaped to acquire objects during reach. Firing continued through the period of object acquisition and then subsided as manipulatory behaviors such as lift began. Holding and relaxation of grasp resulted in inhibition or return of activity to baseline rates.

DISCUSSION

This report is the first study to directly quantify the firing patterns of hand manipulation neurons in both area 5 and AIP/7b of the same animals during prehension. Our digital video methodology allowed us to correlate neuronal firing patterns in the hand representation of PPC with skilled behaviors performed during a trained grasp-and-lift task. Hand actions in the task were divided into well-defined stages that encompassed reach, grasp, manipulation, and release of the test objects. We found marked similarities in responses of neurons recorded in the SPL and IPL during these behaviors. In both areas, object acquisition evoked the strongest responses. Eight-eight percent of area 5 neurons and 77% of AIP/7b neurons fired at their highest rates during at least one of the initial three stages of the task. In this period, the hand was brought to the object, touched, and grasped it. Although each of the animals we studied had a favorite method for grasping and holding the objects, their firing patterns followed a similar time course.

Neural activity in PPC began at or before the onset of reach. Eighty-three percent of task-related neurons in area 5 and 72% in AIP/7b were activated at the start of approach, showing significant increases in firing over baseline; similar proportions of neurons maintained elevated firing rates as the hand contacted the object and grasped it. Our kinematic analyses of the video images showed that as the hand was projected toward the object, it was rotated to a suitable orientation for efficient grasp, and the fingers opened to encompass the object in a smooth and rapid manner. Neural firing rates rose steadily during this period of hand preshaping, and typically peaked at contact. As discussed in the following text, we propose that activity during the approach stage reflects integration of visual information about the object, somatosensory information from the hand, and motor commands from frontal motor areas specifying the type of movement necessary to achieve the goal of grasping and manipulating that object.

Tactile contact with the object provided the strongest signal in the population. These high firing rates appeared to have both a sensory and a motor function. At the moment of contact, view of the object during reach was combined with the feel of the object, as the hand slid over the surface to grasp it. Object features such as surface curvature, edges, and texture were detected by mechanoreceptors in the hand and transmitted centrally to S-I cortex, and eventually to

neurons in the hand representation of area 5, many of which had tactile receptive fields on the hand (see legend Fig. 9). This information provided feedback to the animal concerning the accuracy of the reach and helped guide the fingers to the preferred location(s) for grasping and subsequent manipulation. In cases where the animal missed the target, or contacted an incorrect object, the tactile information provided a signal to abort the current action and/or initiate corrective maneuvers to achieve the desired goal. In addition, some of the neurons illustrated in the report had receptive fields on the dorsum of the fingers and hand, allowing them to sense flexion movements as objects were grasped (Edin and Abbs 1991;Edin and Johansson 1995).

Translational movements of the hand over the object ceased during the grasp stage. Motor activity occurred primarily in the distal hand muscles as grip forces increased to secure the object in the hand (Brochier et al. 2004; Picard and Smith 1992). Neuronal firing rates in PPC decreased in amplitude as grasp was secured, demarcating object acquisition from subsequent manipulatory hand actions.

The shift in task goals and motor behavior from actions of the fingers to more proximal parts of the hand and arm during the lift, hold, and lower stages was accompanied by a dramatic decrease in PPC firing rates. Brochier et al. (2004) demonstrated that patterns of muscle activation in the monkey differed substantially during reach and grasp with the major transition occurring during the contact stage when the hand was placed directly on the object and grasp initiated. During manipulatory actions, the hand and object formed a functional unit, moving together to new positions. The change in the pattern of hand muscle activity was paralleled by clear alterations in PPC firing patterns particularly in area 5. Maintained grasp during holding was ineffective in driving PPC neurons as few were excited, and > 40% were inhibited during this period. Inhibition also predominated in the late stages as grip was relaxed and the object discarded from the hand.

Perhaps the most striking finding is the strong similarity of firing patterns between neurons in SPL and IPL under the same task conditions. Differences in responses observed in area 5 and AIP/7b were subtle and related primarily to the response duration. AIP neurons tended to be activated slightly earlier than those in area 5 and elevated firing rates persisted longer. Half of the population of AIP/7b neurons studied were classified as broadly tuned, showing no significant difference in mean firing rates in three or more successive stages, suggesting that their firing patterns may signal a comprehensive action sequence, rather than specific components of the task. Firing rates of area 5 neurons were more narrowly focused on acquisition or grasping actions, although there was considerable overlap in response duration with that recorded in AIP/7b in the same animals.

These findings together suggest that hand manipulation neurons on both sides of the IPS participate in a sensorimotor network involved in grasp planning, prediction of sensory stimulation, and monitoring of appropriate execution of the desired actions. Firing patterns of PPC neurons described in this report appear to reflect the internal motor commands needed to accomplish task goals, and the sensory events resulting from self-generated movement. Increases in firing rate seem best correlated with the preparation of specific actions. The external tactile stimulation of the hand by the grasped object and the signaling of specific object features appeared to be of secondary importance in modulating the activity of these PPC neurons. Somatosensory feedback from the hand instead seemed to signal the accomplishment of the desired actions when successful or provided an error signal for corrective maneuvers when it failed.

Our findings confirm and extend previous studies of hand manipulation neurons in PPC. Mountcastle and co-workers (1975) first described hand manipulation neurons in both the anterior and posterior banks of the IPS (areas 5 and 7) that responded to hand actions in

immediate extrapersonal space “aimed at securing for the animal an object he desires, such as food when he is hungry; or, as in our experimental paradigm, contacting a switch or pulling a lever that provides fluid when he is thirsty.” Winkling behaviors, such as foraging for raisins in small containers, were difficult to quantify with the equipment available at that time. Similar anecdotal reports of goal directed responses to hand movements in area 7b were provided by Leinonen et al. (1979). Iwamura and co-workers reported shape-specific responses in the anterior bank of IPS during spontaneous grasp of random objects such as fruits, rulers, or blocks (Iwamura and Tanaka 1978; Iwamura et al. 1985, 1995). However, they did not measure kinematic actions of the hand or test the same object repeatedly.

Sakata and co-workers performed the first systematic studies of hand manipulation neurons in PPC using a trained prehension task (Murata et al. 2000; Sakata et al. 1995; Taira et al. 1990). They demonstrated that AIP neurons were strongly activated during reach and grasp behaviors, and these responses were often enhanced by view of the object. Although they did not specifically distinguish reach, grasp, and pulling actions in the neural responses, inspection of their data suggests a similar time course to the responses quantified in our studies. Peak activity in their PSTHs appears to have occurred midway between the start of reach and the onset of hold, but response timing varied in the limited data set illustrated in their reports.

Recent studies by Murata and co-workers (Murata et al. 1997, 2000; Raos et al. 2004, 2006) analyzed the influence of object properties on neurons recorded in area AIP, their primary projection targets in area F5 of ventral premotor cortex, and projection sites in area F2vr of hand and wrist neurons in the SPL. Neurons in all three areas did not distinguish the geometry of objects grasped using the same or similar hand postures but were instead influenced by the type of manipulatory action performed by the hand, and the presence or absence of visual guidance. They concluded that these circuits are involved in the creation of “pragmatic representations” of objects in which their intrinsic properties (size, shape, and orientation) are encoded in terms of the hand postures normally used to grasp them. Because neurons in area AIP responded to both direct view of an object to be grasped and to the actual performance of grasp, they were postulated to be involved in the sensorimotor transformations needed for grasping (reviewed in Fogassi and Luppino 2005; Jeannerod et al. 1995). Our data from both the SPL and IPL are consistent with these ideas and provide additional support for them. For example, the data in Fig. 5 show that when rectangular and round objects were grasped with the same posture, the neuronal firing patterns were similar in time course and amplitude. However, when the hand posture and contact area on the skin differed, neural responses to the same object were also modified (Debowy et al. 2004). A more comprehensive analysis of the effect of object features in our task is the subject of a future report.

Neurons in PPC serve a sensorimotor role

Traditionally, area 5 was thought to be a higher-order somatosensory area that processed tactile input for the purpose of exteroception and object recognition (Ageranioti-Bélanger and Chapman 1992; Darian-Smith et al. 1984; Felleman and Van Essen 1991; Iwamura and Tanaka 1978; Iwamura et al. 1995; Koch and Fuster 1989) and processed proprioceptive signals for perception of integrated body postures (Duffy and Burchfiel 1971; Sakata et al. 1973). This notion was supported by anatomical evidence that S-I cortex provided the principal inputs to area 5, particularly from area 2 (Jones and Powell 1969, 1970; Pearson and Powell 1985). Although many of the physiological studies attributed recording sites in the superior bank of the IPS to area 2, anatomists such as Pandya and Selzer (1982), Pons et al. (1985) and Lewis et al. (1999) included this region in Brodmann’s area 5, calling it area PEa or 5v. Interestingly, most of the complex tactile responses reported by physiologists were recorded during active hand movements, such as grasping objects or palpating textured surfaces, in which such behaviors were rewarded.

The discovery by Mountcastle and co-workers (1975) of the role of areas 5 and 7 in motor control and subsequent studies by others have transformed the functional view of PPC from one of higher-order somatosensory and visual processing in a hierarchical network into a complex system of interconnected parietal and frontal loops that couple perceptions to action to accomplish specific goals (reviewed in Andersen and Buneo 2002; Andersen et al. 1997; Battaglia-Mayer et al. 2003; Buneo and Andersen 2006; Burnod et al. 1999; Caminiti et al. 1996, [1998]; Colby 1998; Fogassi and Luppino 2005; Freund 2001; Ghosh and Gattera 1995; Kalaska et al. 1997; Luppino et al. 1999; Matelli et al. 1986, 1998; Rizzolatti et al. 1997; Wise et al. 1997). Perhaps the most important original insight came from comparative studies of frontal motor areas and neurons in area 5 by Kalaska and co-workers (Crammond and Kalaska 1989; Kalaska and Crammond 1995; Kalaska et al. 1983, 1990) and Burbaud et al. (1991), who demonstrated that neuronal activity in MI, PMd, and area 5 overlapped in time at the onset of reach and that area 5 neurons were directionally tuned during movements and postures. In addition, studies in deafferented monkeys by Seal et al. (Seal and Commenges 1985; Seal et al. 1982) indicated that area 5 neurons respond to reaching movements in the absence of somatosensory feedback. These findings led to the proposal that area 5 receives convergent central and peripheral signals that allow it to compare central motor commands with peripheral sensory feedback during task performance. These circuits could provide a network for updating on-going actions as they proceed, a function described as a “sequence of sensorimotor coordinate transformations between a signal of spatial location and a pattern of muscle activity” (Kalaska et al. 1997). The representation of actions of the hand in PPC in terms of task goals is also supported by recent studies of prehension by Tunik and coworkers (2005) using transcranial magnetic stimulation (TMS) applied over the human anterior intraparietal sulcus (aIPS). Corrective alteration of grip aperture and/or hand rotation was slowed or impeded by TMS applied to aIPS within 65 ms of object perturbation in normal subjects, suggesting that this brain region plays a role in dynamic error correction of hand movements.

Studies of medial regions of area 5 by various investigators indicated that it played a major role in sensorimotor transformations in which tactile, proprioceptive, and visual signals were combined with central motor commands to generate a plan of action directed toward particular targets in space, and subsequently monitor its execution (Andersen and Buneo 2002; Andersen et al. 1997; Batista and Andersen 2001; Batista et al. 1999; Battaglia-Mayer et al. 2000; Buneo and Andersen 2006; Fattori et al. 2004; Ferraina et al. 1997, [2001]; Galletti et al. 1993, [1997], [2003]; Kalaska and Crammond 1995; Kalaska et al. 1983; Lacquiniti et al. 1995; Snyder et al. 1998). Neurons in the SPL were shown to play an important role in perception of the body and its relation to external space during reaching. Reach targets were encoded by neurons in the shoulder representation of area 5, the parietal reach region (PRR) including areas MIP and PEc, and areas V6, V6A and 7m on the medial surface of the hemisphere. Their firing rates increased as the hand was projected toward a target before it was touched; goal-related firing also occurred in these areas during motor planning in instructed delay tasks. Actions of the arm appear to be represented in a variety of coordinate systems along the SPL including eye-centered, arm-centered, head-centered, and hand-centered reference frames or combinations of these expressed as gain fields.

The findings presented in our report indicate that neurons in the hand region of area 5 should be included in this sensorimotor guidance network as they may enable the coordination of reach with grasping actions as the hand arrives at the target. Strong interconnections between rostral and caudal subregions of the SPL (Lewis and Van Essen 2000b; Pandya and Selzer 1982; Selzer and Pandya 1980) provide an anatomical pathway for coordination of different limb segments during goal-directed hand behaviors. Indeed, microinjection of Fast blue dye at the crown of the SPL in one of our animals confirmed such horizontal linkages between the physiologically identified hand representation and more medial regions of area 5 (unpublished observations).

We propose that the task-related responses in the hand representation of PPC are sensorimotor, linked to the progress of object acquisition. These responses appear to signal actions and their planning not just the movements of the hand or the sensory cues from the hand-object interface. We found that each attempt to acquire a new object in the hand was accompanied by a robust response from the majority of analyzed PPC neurons. However, the hand postures involved in object acquisition did not evoke increased activity from PPC neurons when they were assumed as part of other behaviors such as inspection of the fingernails. Similarly, reaches out into space without attempts at grasping an object usually did not drive cells as strongly as reach and grasp behaviors. In contrast, PPC cells responses were altered when the animal incorrectly targeted the reach and the hand grasped at the space adjacent to the object, missing the desired goal. The subsequent corrective movements elicited a second discrete acquisition response as the animal re-extended its digits and initiated a lateral reach to the knob. PPC neurons also responded to acquisition behaviors even when objects were grasped but not manipulated, suggesting that object acquisition was their principal function irrespective of subsequent motor intentions. Finally, responses were frequently attenuated when the animal regrasped the same object without reaching.

By the same token, tactile cues alone were insufficient stimuli in isolation from the proper behavioral context. Tapping against the knobs or resting the hand without grasping the object failed to excite neurons that responded robustly as the hand was positioned on it for grasping. Tactile input at contact appeared to confirm that the intended goal of acquisition had been achieved. Later in the task, as applied grip and load forces were increased, somesthetic inputs suppressd activity of PPC neurons.

Taken together, our data indicate that responses of hand manipulation neurons in the lateral portion of PPC are not purely sensory or kinematic in nature but instead depend on their motor context. The early increase in firing during approach probably reflects efference copy of motor signals related to upcoming reach and grasp actions generated in frontal motor regions such as premotor cortex and MI. The motor signals may be integrated with visual and somatosensory inputs from area LIP and area 2, respectively (Jones and Powell 1969, 1970; Nakamura et al. 2001; Pearson and Powell 1985), as well as with reciprocal connections between area 5 and 7b (Cavada and Goldman-Rakic 1989a; Neal et al. 1986, 1987). Feed-forward connections from area 5, AIP, and 7b may, in turn, provide additional excitatory inputs to premotor areas F5, F4, and F2vr. This sensorimotor loop would allow planning of acquisition to be informed by available sensory cues, such as the current posture of the hand or the sight of object dimensions. This sensorimotor circuit also could monitor the accurate execution of the motor plan, by detecting proprioceptive and tactile signals associated with goal completion or motor errors.

Acknowledgments

We thank Daniel J. Debowy for many contributions to these studies and A. Harris and M. Natiello for skilled technical support. We are most appreciative of the collaborative efforts of Dr. Edward G. (Ted) Jones in histological analyses of one of the animals used in this study; 3-D reconstructions from frozen block face images of the brain can be found at his website www.brain-maps.org. We are grateful to Drs. Daniel Gardner, Michael E. Goldberg, Eric J. Lang, Rodolfo R. Llinás, and John I. Simpson for many helpful comments and criticisms of earlier versions of this report.

GRANTS

Major funding for this study has been provided by National Institute of Neurological Diseases and Stroke Grant R01 NS-11862 and Human Brain Project Research Grant R01 NS-44820 funded jointly by the National Institute of Neurological Diseases and Stroke, National Institute of Mental Health, and the National Institute of Aging.

References

Ageranioti-Bélanger SA, Chapman CE. Discharge properties of neurones in the hand area of primary somatosensory cortex in monkeys in relation to the performance of an active tactile discrimination task. II. Area 2 as compared to areas 3b and 1. Exp Brain Res 1992;91:207–228. [PubMed: 1459224]

Andersen RA, Buneo CA. Intentional maps in posterior parietal cortex. Annu Rev Neurosci 2002;25:189–220. [PubMed: 12052908]

Andersen RA, Snyder LH, Bradley DC, Xing J. Multimodal representation of space in the posterior parietal cortex and its use in planning movements. Annu Rev Neurosci 1997;20:303–330. [PubMed: 9056716]

Batista AP, Andersen RH. The parietal reach region codes the next planned movement in a sequential reach task. J Neurophysiol 2001;85:539–544. [PubMed: 11160491]

Batista AP, Buneo CA, Snyder LH, Andersen RA. Reach plans in eye-centered coordinates. Science 1999;285:257–260. [PubMed: 10398603]

Babu KS, Debowy DJ, Ghosh S, Hu EH, Natiello M, Harris A, Gardner EP. Spike burst analysis: a tool for analysing spontaneous prehension behaviors recorded with digital video. Soc Neurosci Abstr 2000;26:2202.

Battaglia-Mayer A, Ferraina S, Mitsuda T, Marconi B, Genovesio A, Onorati P, Lacquaniti F, Caminiti R. Early coding of reaching in the parieto-occipital cortex. J Neurophysiol 2000;83:2374–2391. [PubMed: 10758140]

Battaglia-Mayer A, Caminiti R, Lacquaniti F, Zago M. Multiple levels of representation of reaching in the parieto-frontal network. Cereb Cortex 2003;13:1009–1022. [PubMed: 12967918]

Binkofski F, Buccino G, Stephan KM, Rizzolatti G, Seitz RJ, Freund HJ. A parieto-premotor network for object manipulation: evidence from neuroimaging. Exp Brain Res 1999;128:210–213. [PubMed: 10473761]

Binkofski F, Dohle C, Posse S, Stephan K, Hefter H, Seitz R, Freund H. Human anterior intraparietal area subserves prehension: a combined lesion and functional MRI activation study. Neurology 1998;50:1253–1259. [PubMed: 9595971]

Brochier T, Spinks RL, Umilta MA, Lemon RN. Patterns of muscle activity underlying object-specific grasp by the Macaque monkey. J Neurophysiol 2004;92:1770–1782. [PubMed: 15163676]

Buneo CA, Andersen RA. The posterior parietal cortex: Sensorimotor interface for the planning and online control of visually guided movements. Neuropsychologia 2006;44:2594–2606. [PubMed: 16300804]

Burbaud P, Doegle C, Gross C, Bioulac B. A quantitative study of neuronal discharge in areas 5, 2 and 4 of the monkey during fast arm movements. J Neurophysiol 1991;66:429–443. [PubMed: 1774580]

Burnod Y, Baraduc P, Battaglia-Mayer A, Guigon E, Koechlin E, Ferraina S, Lacquaniti F, Caminiti R. Parieto-frontal coding of reaching: an integrated framework. Exp Brain Res 1999;129:325–346. [PubMed: 10591906]

Caminiti R, Ferraina S, Johnson PB. The sources of visual information to the primate frontal lobe: a novel role for the superior parietal lobule. Cereb Cortex 1996;6:319–328. [PubMed: 8670660]

Caminiti R, Ferraina S, Mayer AB. Visuomotor transformations: early cortical mechanisms of reaching. Curr Opin Neurobiol 1998;8:753–761. [PubMed: 9914239]

Cavada C, Goldman-Rakic P. Posterior parietal cortex in rhesus monkey. I. Parcellation of areas based on distinctive limbic and sensory corticocortical connections. J Comp Neurol 1989a;287:393– 421. [PubMed: 2477405]

Cavada C, Goldman-Rakic P. Posterior parietal cortex in rhesus monkey. II. Evidence for segregated corticocortical networks linking sensory and limbic areas with the frontal lobe. J Comp Neurol 1989b; 287:422– 445. [PubMed: 2477406]

Chieffi S, Gentilucci M. Coordination between the transport and the grasp component during prehension movements. Exp Brain Res 1993;94:471– 477. [PubMed: 8359261]

Colby CL. Action-oriented spatial reference frames in cortex. Neuron 1998;20:15–24. [PubMed: 9459438]

Crammond DJ, Kalaska JF. Neuronal activity in primate parietal cortex area 5 varies with intended movement direction during an instructed-delay period. Exp Brain Res 1989;76:458–462. [PubMed: 2767196]

Culham JC, Danckert SL, DeSouza JF, Gati JS, Menon RS, Goodale MA. Visually guided grasping produces fMRI activation in dorsal but not ventral stream brain areas. Exp Brain Res 2003;153:180–189. [PubMed: 12961051]

Darian-Smith, I.; Goodwin, A.; Sugitani, M.; Heywood, J. The tangible features of textured surfaces: their representation in the monkey's somatosensory cortex. In: Edelman, G.; Gall, WE.; Cowan, WM., editors. Dynamic Aspects of Neocortical Function. New York: Wiley; 1984. p. 475-500.

Debowy, DJ.; Babu, KS.; Hu, EH.; Natiello, M.; Reitzen, S.; Chu, M.; Sakai, J.; Gardner, EP. New applications of digital video technology for neurophysiological studies of hand function. In: Nelson, R., editor. The Somatosensory System: Deciphering the Brain's Own Body Image. Boca Raton FL: CRC; 2002. p. 219-241.

Debowy DJ, Babu KS, Bailey JM, Brown AS, Hall AL, Herzlinger M, Gardner EP. Object feature selectivity of posterior parietal cortical (PPC) neurons during prehension. Soc Neurosci Abstr 2004;30:59.2.

Debowy DJ, Ghosh S, Ro JY, Gardner EP. Comparison of neuronal firing rates in somatosensory and posterior parietal cortex during prehension. Exp Brain Res 2001;137:269–291. [PubMed: 11355375]

DiCarlo JJ, Lane SW, Hsiao SS, Johnson KO. Marking microelectrode penetrations with fluorescent dyes. J Neurosci Methods 1996;64:75–81. [PubMed: 8869487]

Duffy FH, Burchfiel JL. Somatosensory system: organizational hierarchy from single units in monkey area 5. Science 1971;172:273–275. [PubMed: 4994137]

Edin BB, Abbs JH. Finger movement responses of cutaneous mechanoreceptors in the dorsal skin of the human hand. J Neurophysiol 1991;65:657–670. [PubMed: 2051199]

Edin BB, Johansson RN. Skin strain patterns provide kinaesthetic information to the human central nervous system. J Physiol 1995;487:243–251. [PubMed: 7473253]

Ehrsson HH, Fagergren A, Jonsson T, Westling G, Johansson RS, Forssberg H. Cortical activity in precision- versus power-grip tasks: an fMRI study. J Neurophysiol 2000;83:528–536. [PubMed: 10634893]

Fattori P, Breveglieri R, Amoroso K, Galletti C. Evidence for both reaching and grasping activity in the medial parieto-occipital cortex of the macaque. Eur J Neurosci 2004;20:2457–2466. [PubMed: 15525286]

Felleman DJ, Van Essen DC. Distributed hierarchical processing in the primate cerebral cortex. Cereb Cortex 1991;1:1– 47. [PubMed: 1822724]

Ferraina S, Battaglia-Mayer A, Genovesio A, Marconi B, Onorati P, Caminiti R. Early coding of visuomanual coordination during reaching in parietal area PEc. J Neurophysiol 2001;85:462– 467. [PubMed: 11152747]

Ferraina S, Johnson PB, Garasto MR, Battaglia-Mayer A, Ercolani L, Bianchi L, Lacquaniti F, Caminiti R. Combination of hand and gaze signals during reaching: activity in parietal area 7m of the monkey. J Neurophysiol 1997;77:1034–1038. [PubMed: 9065868]

Fogassi L, Luppino G. Motor functions of the parietal lobe. Curr Opin Neurobiol 2005;15:626–631. [PubMed: 16271458]

Fogassi L, Gallese V, Buccino G, Craighero L, Fadiga L, Rizzolatti G. Cortical mechanism for the visual guidance of hand grasping movements in the monkey: a reversible inactivation study. Brain 2001;124:571–586. [PubMed: 11222457]

Freund H-J. The parietal lobe as sensorimotor interface: a perspective from clinical and neuroimaging data. Neuroimage 2001;14:S142–146. [PubMed: 11373146]

Frey SH, Vinton D, Norlund R, Grafton ST. Cortical topography of human anterior intraparietal cortex active during visually guided grasping. Cogn Brain Res 2005;23:397–405.

Gallese V, Murata A, Kaseda M, Niki N, Sakata H. Deficit of hand preshaping after muscimol injection in monkey parietal cortex. Neuroreport 1994;5:1525–1529. [PubMed: 7948854]

Galletti C, Battaglini PP, Fattori P. Parietal neurons encoding spatial locations in craniotopic coordinates. Exp Brain Res 1993;96:221–229. [PubMed: 8270019]

Galletti C, Fattori P, Kutz DF, Battaglini PP. Arm movement related neurons in the visual area V6A of the macaque superior parietal lobule. Eur J Neurosci 1997;9:410–413. [PubMed: 9058060]

Galletti C, Gamberini M, Breveglieri R, Fattori P. Role of the medial parieto-occipital cortex in the control of reaching and grasping movements. Exp Brain Res 2003;153:158–170. [PubMed: 14517595]

Gardner EP, Costanzo RM. Spatial integration of multiple-point stimuli in primary somatosensory cortical receptive fields of alert monkeys. J Neurophysiol 1980;43:420–443. [PubMed: 6770053]

Gardner EP, Debowy D, Ro JY, Ghosh S, Babu KS. Sensory monitoring of prehension in the parietal lobe: a study using digital video. Behav Brain Res 2002;135:213–224. [PubMed: 12356452]

Gardner EP, Ro JY, Debowy D, Ghosh S. Facilitation of neuronal firing patterns in somatosensory and posterior parietal cortex during prehension. Exp Brain Res 1999;127:329–354. [PubMed: 10480270]

Ghosh S, Gattera R. A comparison of the ipsilateral cortical projections to the dorsal and ventral subdivisions of the macaque premotor cortex. Somatosens Mot Res 1995;12:359–376. [PubMed: 8834308]

Goodale MA, Westwood DA. An evolving view of duplex vision: separate but interacting cortical pathways for perception and action. Curr Opin Neurobiol 2004;14:203–211. [PubMed: 15082326]

Grafton ST, Fagg AH, Woods RP, Arbib MA. Functional anatomy of pointing and grasping in humans. Cereb Cortex 1996;6:226–237. [PubMed: 8670653]

Hyvärinen J. Regional distribution of functions in parietal association area 7 of the monkey. Brain Res 1981;206:287–303. [PubMed: 7214136]

Iwamura Y, Tanaka M. Postcentral neurons in hand region of area 2: their possible role in the form discrimination of tactile objects. Brain Res 1978;150:662– 666. [PubMed: 98206]

Iwamura Y, Tanaka M, Sakamoto M, Hikosaka O. Functional surface integration, submodality convergence, and tactile feature detection in area 2 of the monkey somatosensory cortex. Exp Brain Res Suppl 1985;10:44–58.

Iwamura Y, Tanaka M, Sakamoto M, Hikosaka O. Rostrocaudal gradients in neuronal receptive field complexity in the finger region of the alert monkey's postcentral gyrus. Exp Brain Res 1993;92:360–368. [PubMed: 8454001]

Iwamura Y, Tanaka M, Hikosaka O, Sakamoto M. Postcentral neurons of alert monkeys activated by the contact of the hand with objects other than the monkey's own body. Neurosci Lett 1995;186:127–130. [PubMed: 7777180]

Jeannerod M. The formation of finger grip during prehension: a cortically mediated visuomotor pattern. Behav Brain Res 1986;19:99–116. [PubMed: 3964409]

Jeannerod M. The hand and the object: the role of posterior parietal cortex in forming motor representations. Can J Physiol Pharmacol 1994;72:535–541. [PubMed: 7954083]

Jeannerod M, Arbib MA, Rizzolatti G, Sakata H. Grasping objects: the cortical mechanisms of visuomotor transformation. Trends Neurosci 1995;18:314–320. [PubMed: 7571012]

Jeannerod M, Decety J, Michel F. Impairment of grasping movements following a bilateral posterior parietal lesion. Neuropsychologia 1994;32:369–380. [PubMed: 8047246]

Jones EG, Powell TPS. Connexions of the somatic sensory cortex of the rhesus monkey. I. Ipsilateral cortical connexions. Brain 1969;92:477–502. [PubMed: 4979846]

Jones EG, Powell TPS. An anatomical study of converging sensory pathways within the cerebral cortex of the monkey. Brain 1970;93:793–820. [PubMed: 4992433]

Kalaska JF. Parietal cortex area 5 and visuomotor behavior. Can J Physiol Pharmacol 1996;74:483–498. [PubMed: 8828894]

Kalaska JF, Crammond DJ. Deciding not to GO: neural correlates of response selection in a GO/NOGO task in primate premotor and parietal cortex. Cereb Cortex 1995;5:410–428. [PubMed: 8547788]

Kalaska JF, Caminiti R, Georgopoulos AP. Cortical mechanisms related to the direction of two-dimensional arm movements: relations in parietal area 5 and comparison with motor cortex. Exp Brain Res 1983;51:247–260. [PubMed: 6617794]

Kalaska JF, Cohen DAD, Prud'Homme MJL, Hyde ML. Parietal area 5 neuronal activity encodes movement kinematics, not movement dynamics. Exp Brain Res 1990;80:351–364. [PubMed: 2113482]

Kalaska JF, Scott SH, Cisek P, Sergios LE. Cortical control of reaching movements. Curr Opin Neurobiol 1997 1997;7:849–859.

Koch KW, Fuster JM. Unit activity in monkey parietal cortex related to haptic perception and temporary memory. Exp Brain Res 1989;76:292–306. [PubMed: 2767186]

Kurata K. Corticocortical inputs to the dorsal and ventral aspects of the premotor cortex of macaque monkeys. Neurosci Res 1991;12:263–280. [PubMed: 1721118]

Lacquaniti F, Guigon E, Bianchi L, Ferraina S, Caminiti R. Representing spatial information for limb movement: role of area 5 in the monkey. Cereb Cortex 1995;5:391–409. [PubMed: 8547787]

LaMotte RH, Acuña C. Defects in accuracy of reaching after removal of posterior parietal cortex in monkeys. Brain Res 1978;139:309–326. [PubMed: 414819]

Leinonen L, Hyvärinen J, Nyman G, Linnankowski I. Functional properties of neurons in lateral part of associative area 7 in awake monkey. Exp Brain Res 1979;34:299–320. [PubMed: 105918]

Lewis JW, Burton H, Van Essen DC. Anatomical evidence for the posterior boundary of area 2 in the macaque monkey. Somatosens Mot Res 1999;16:382–390. [PubMed: 10632034]

Lewis JW, Van Essen DC. Mapping of architectonic subdivisions in the macaque monkey, with emphasis on parieto-occipital cortex. J Comp Neurol 2000a;428:79–111. [PubMed: 11058226]

Lewis JW, Van Essen DC. Corticocortical connections of visual, sensorimotor, and multimodal processing areas in the parietal lobe of the macaque monkey. J Comp Neurol 2000b;428:112–137. [PubMed: 11058227]

Luppino G, Murata A, Govoni P, Matelli M. Largely segregated parieto-frontal connections linking rostral intraparietal cortex (areas AIP and VIP) and the ventral premotor cortex (areas F5 and F4). Exp Brain Res 1999;128:181–187. [PubMed: 10473756]

Matelli M, Camarda R, Glickstein M, Rizzolatti G. Afferent and efferent projections of the inferior area 6 in the macaque monkey. J Comp Neurol 1986;251:281–298. [PubMed: 3021823]

Matelli M, Govoni P, Galletti C, Kutz DF, Luppino G. Superior area 6 afferents from the superior parietal lobule in the macaque monkey. J Comp Neurol 1998;402:327–352. [PubMed: 9853903]

Milner, AD.; Goodale, MA. The Visual Brain in Action. Oxford, UK: Oxford Univ. Press; 1995.

Mountcastle VB. The parietal system and some higher brain functions. Cereb Cortex 1995;5:377–390. [PubMed: 8547786]

Mountcastle VB, Lynch JC, Georgopoulos A, Sakata H, Acuna C. Posterior parietal association cortex of the monkey: command functions for operations within extrapersonal space. J Neurophysiol 1975;38:871–908. [PubMed: 808592]

Murata A, Fadiga L, Fogassi L, Gallese V, Raos V, Rizzolatti G. Object representation in the ventral premotor cortex (area F5) of the monkey. J Neurophysiol 1997;78:2226–2230. [PubMed: 9325390]

Murata A, Gallese V, Kaseda M, Sakata H. Parietal neurons related to memory-guided hand manipulation. J Neurophysiol 1996;75:2180–2186. [PubMed: 8734616]

Murata A, Gallese V, Luppino G, Kaseda M, Sakata H. Selectivity for the shape, size and orientation of objects for grasping in neurons of monkey parietal area AIP. J Neurophysiol 2000;83:2580–2601. [PubMed: 10805659]

Nakamura H, Kuroda T, Wakita M, Kusunoki M, Kato A, Mikami A, Sakata H, Itoh K. From three-dimensional space vision to prehensile hand movements: the lateral intraparietal area links the area V3A and the anterior intraparietal area in macaque monkeys. J Neurosci 2001;21:8174–8187. [PubMed: 11588190]

Neal JW, Pearson RCA, Powell TPS. The organization of the corticocortical projection of area 5 upon area 7 in the parietal lobe of the monkey. Brain Res 1986;381:164–167. [PubMed: 3756496]

Neal JW, Pearson RCA, Powell TPS. The corticocortical connections of area 7b, PF, in the parietal lobe of the monkey. Brain Res 1987;419:341–346. [PubMed: 2445426]

Pandya DN, Seltzer B. Intrinsic connections and architectonics of posterior parietal cortex in the rhesus monkey. J Comp Neurol 1982;204:196–210. [PubMed: 6276450]

Paulignan, Y.; Jeannerod, M. Prehension movements: The visuomotor channels hypothesis revisited. In: Wing, AM.; Haggard, P.; Flanagan, JR., editors. Hand and Brain. San Diego, CA: Academic Press; 1996. p. 265-282.

Pause M, Freund H-J. Role of the parietal cortex for sensorimotor transformation. Evidence from clinical observations. Brain Behav Evol 1989;33:136–140. [PubMed: 2758292]

Pause M, Kunesch E, Binkofski F, Freund H-J. Sensorimotor disturbances in patients with lesions of the parietal cortex. Brain 1989;112:1599–1625. [PubMed: 2598000]

Pearson RCA, Powell TPS. The projection of the primary somatic sensory cortex upon area 5 in the monkey. Brain Res Rev 1985;9:89–107.

Petrides M, Pandya DN. Projections to the frontal cortex from the posterior parietal region in the rhesus monkey. J Comp Neurol 1984;228:105–116. [PubMed: 6480903]

Picard N, Smith AM. Primary cortical activity related to the weight and texture of grasped objects in the monkey. J Neurophysiol 1992;68:1867–1881. [PubMed: 1479450]

Pons TP, Garraghty PE, Cusick CG, Kaas JH. The somatotopic organization of area 2 in macaque monkeys. J Comp Neurol 1985;241:445–466. [PubMed: 4078042]

Raos V, Umilta' MA, Gallese V, Fogassi L. Functional properties of grasping-related neurons in the dorsal premotor area F2 of the macaque monkey. J Neurophysiol 2004;92:1990–2002. [PubMed: 15163668]

Raos V, Umilta' MA, Murata A, Fogassi L, Gallese V. Functional properties of grasping-related neurons in the ventral premotor area F5 of the macaque monkey. J Neurophysiol 2006;95:709–729. [PubMed: 16251265]

Reitzen SD, Debowy DJ, Gardner EP. Kinematic analyses of prehension in macaques. Soc Neurosci Abstr 2004;30:59.3.

Rizzolatti G, Fogassi L, Gallese V. Parietal cortex: from sight to action. Curr Opin Neurobiol 1997;7:562–567. [PubMed: 9287198]

Ro JY, Debowy D, Lu S, Ghosh S, Gardner EP. Digital video: a tool for correlating neuronal firing patterns with hand motor behavior. J Neurosci Methods 1998;82:215–231. [PubMed: 9700695]

Ro JY, Debowy D, Ghosh S, Gardner EP. Depression of neuronal activity in somatosensory and posterior parietal cortex during prehension. Exp Brain Res 2000;135:1–11. [PubMed: 11104122]

Roy AC, Paulignan Y, Farne A, Jouffrais C, Boussaoud D. Hand kinematics during reaching and grasping in the macaque monkey. Behav Brain Res 2000;117:75–82. [PubMed: 11099760]

Roy A, Paulignan Y, Meunier M, Boussaoud D. Prehension movements in the macaque monkey: effects of object size and location. J Neurophysiol 2002;88:1491–1499. [PubMed: 12205169]

Sakata H, Takaoka A, Hawarasaki A, Shibutani H. Somatosensory properties of neurons in superior parietal cortex (area 5) of the rhesus monkey. Brain Res 1973;64:85–102. [PubMed: 4360893]

Sakata H, Taira M, Murata A, Mine S. Neural mechanisms of visual guidance of hand action in the parietal cortex of the monkey. Cereb Cortex 1995;5:429–438. [PubMed: 8547789]

Sakata H, Taira M, Kusunoki M, Murata A, Tanaka Y. The parietal association cortex in depth perception and visual control of hand action. Trends Neurosci 1997;20:350–357. [PubMed: 9246729]

Sakata H, Taira M, Kusunoki A, Murata A, Tsutsui K-I, Tanaka Y, Shein WN, Miyashita Y. Neural representation of three-dimensional features of manipulation objects with stereopsis. Exp Brain Res 1999;128:160–169. [PubMed: 10473754]

Seal J, Commenges D. A quantitative analysis of stimulus- and movement-related responses in the posterior parietal cortex of the monkey. Exp Brain Res 1985;58:144–153. [PubMed: 3987845]

Seal J, Gross C, Bioulac B. Activity of neurons in area 5 during a simple arm movement in monkey before and after deafferentation of the trained limb. Brain Res 1982;250:229–243. [PubMed: 7171988]

Seltzer B, Pandya DN. Converging visual and somatic sensory cortical input to the intraparietal sulcus of the rhesus monkey. Brain Res 1980;192:339–351. [PubMed: 6769545]

Sherwood A, Lang EJ, Gardner EP. The neuroinformatics digital video toolkit. Soc Neurosci Abstr 2006;32:147.6.

Shikata E, Hamzei F, Glauche V, Koch M, Weiller C, Binkofski F, Buchel C. Functional properties and interaction of the anterior and posterior intraparietal areas in humans. Eur J Neurosci 2003;17:1105–1110. [PubMed: 12653987]

Snyder LH, Batista AP, Andersen RA. Change in motor plan, without a change in the spatial locus of attention, modulates activity in posterior parietal cortex. J Neurophysiol 1998;79:2814–2819. [PubMed: 9582248]

Taira M, Mine S, Georgopoulos AP, Murata A, Sakata H. Parietal cortex neurons of the monkey related to the visual guidance of hand movement. Exp Brain Res 1990;83:29–36. [PubMed: 2073947]

Tanne-Gariepy JT, Rouiller EM, Boussaoud D. Parietal inputs to dorsal versus ventral premotor areas in the macaque monkey: evidence for largely segregated visuomotor pathways. Exp Brain Res 2002;145:91–103. [PubMed: 12070749]

Tunik E, Frey S, Grafton S. Virtual lesions of the anterior intraparietal area disrupt goal-dependent on-line adjustments of grasp. Nat Neurosci 2005;8:505–511. [PubMed: 15778711]

Warren S, Hamalainen HA, Gardner EP. Objective classification of motion-and direction-sensitive neurons in primary somatosensory cortex of awake monkeys. J Neurophysiol 1986;56:598–622. [PubMed: 3783213]

Wise SP, Boussaoud D, Johnson PB, Caminiti R. Premotor and parietal cortex: corticocortical connectivity and combinatorial computations. Annu Rev Neurosci 1997;20:25–42. [PubMed: 9056706]

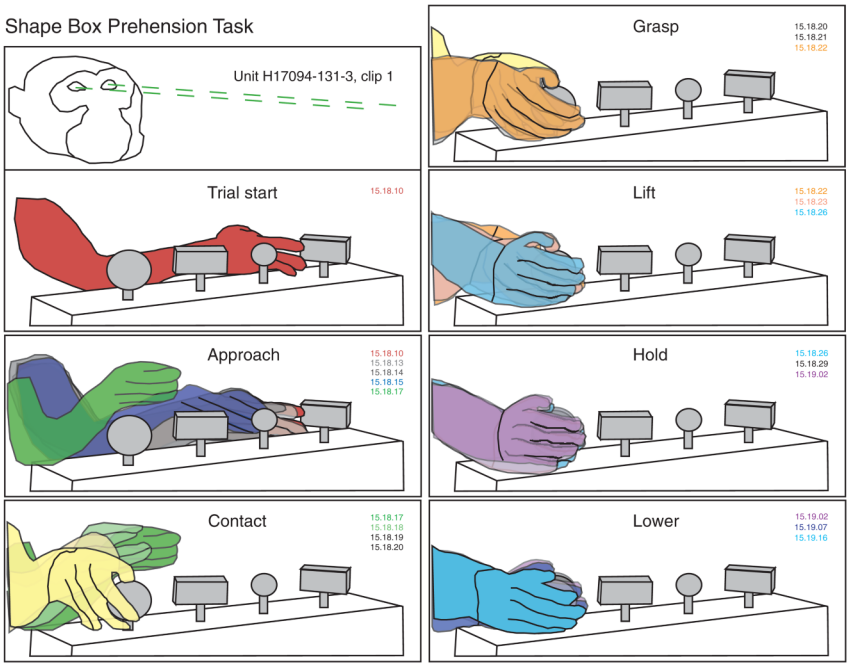

FIG. 1.

Stages of the prehension task traced from sequential digital video images of a lateral reach trial. Labels describe the action performed in the top image of each set. This trial starts with the hand resting on knob 1 (left rectangle). Approach begins as the animal retracts his hand from the knob and lifts the wrist. The hand follows an arc-like path toward the right side of the workspace. Wrist rotation is coordinated with hand preshaping as the hand decelerates and descends near the large round knob. The fingertips contact the knob on its lateral side, and the hand moves downward to grasp it between the fingers and the palm. Once grasp is secured, the knob is rotated, and lift begins. Lowering the knob retraces the same path as lift. Grasp is subsequently relaxed (not shown), ending the trial. Methods for construction of the time series of hand kinematics are summarized in the text. Color matched video time code labels (minute: second:frame) mark the time elapsed between images; frame rate = 29.97 frames/s.

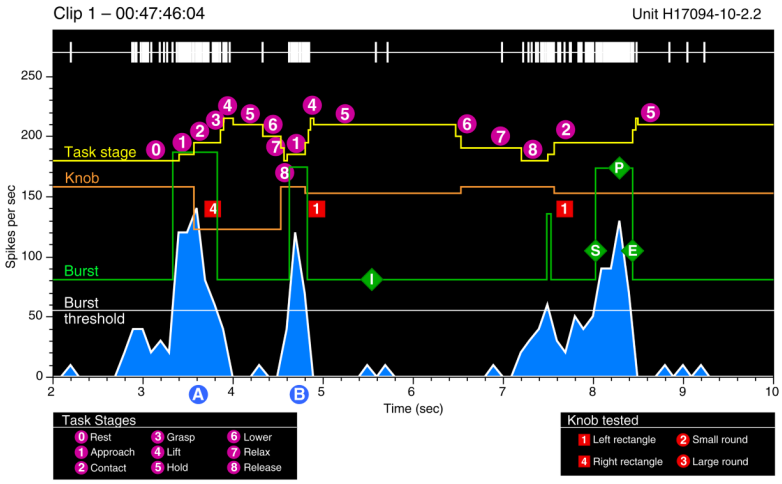

FIG. 2.

Burst-analysis graphs of continuous neural and behavioral activity. This example displays the spike train, continuous firing rate binned in 100-ms intervals (blue graph), and task actions performed during an 8-s period excerpted from a 2.5-min video clip. Yellow task stage trace: each stepped yellow pyramid marks a single trial. Upward deflections denote the start of stages 1– 4; downward deflections mark the onset of stages 5– 8. Orange knob trace: knob location on the shape box and duration of hand contact are depicted as downward pulses that span the contact through lower stages. The pulse amplitude is proportional to the knob distance from the left edge of the box. White burst threshold trace: firing rate set 1 SD above the mean rate during the entire 2.5-min analysis period. Green burst trace: upward deflections mark periods when the firing rate exceeds the burst threshold. The burst amplitude indicates the mean rate during the interval of high activity; in this example, the burst trace is displaced upward by 80 spikes/s for clarity. The neuron responded most vigorously during stages 1–3 on each trial.

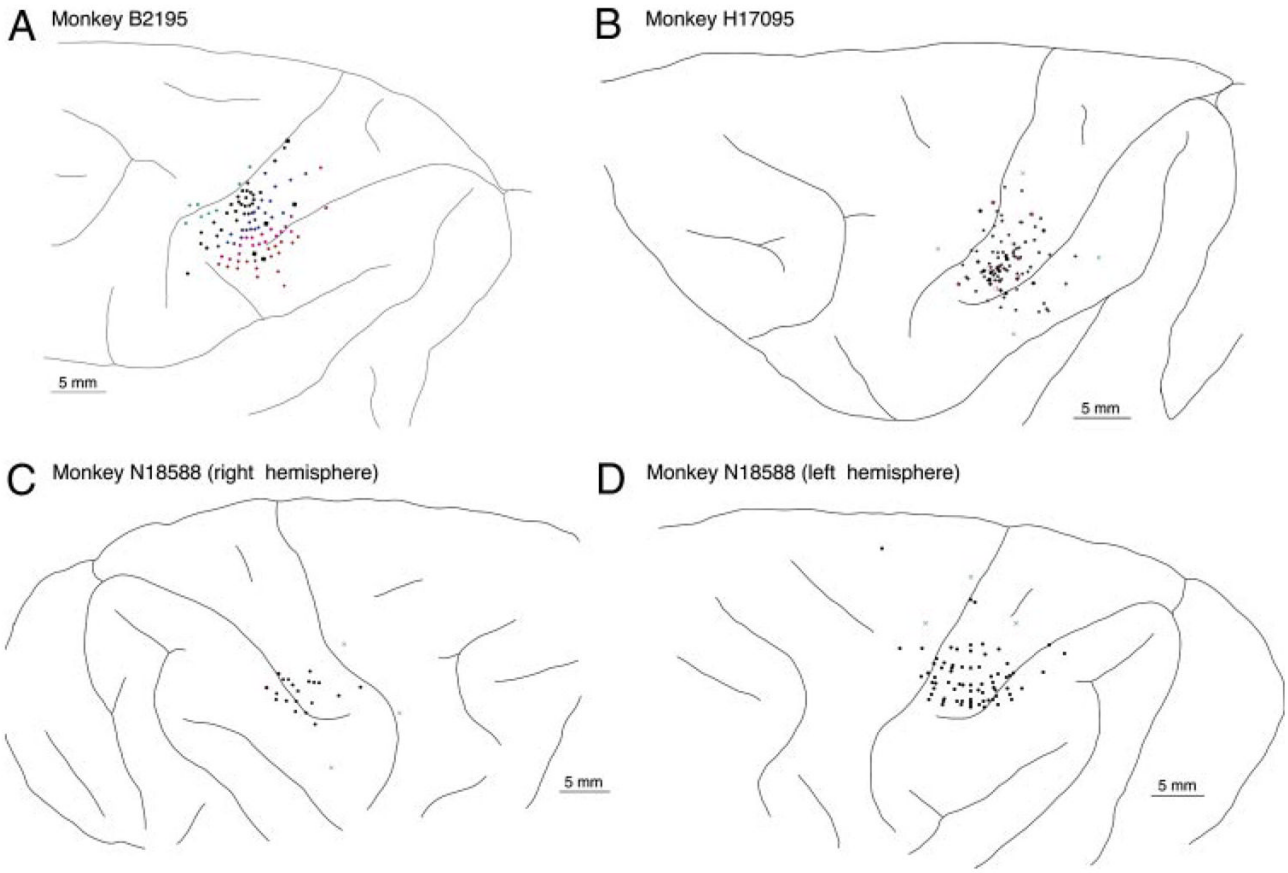

FIG. 3.

Cortical recording sites in the 3 animals studied. Electrode entry points are shown as dots on each brain diagram; they were reconstructed from serial histological sections and dye markers placed at the chamber perimeter.

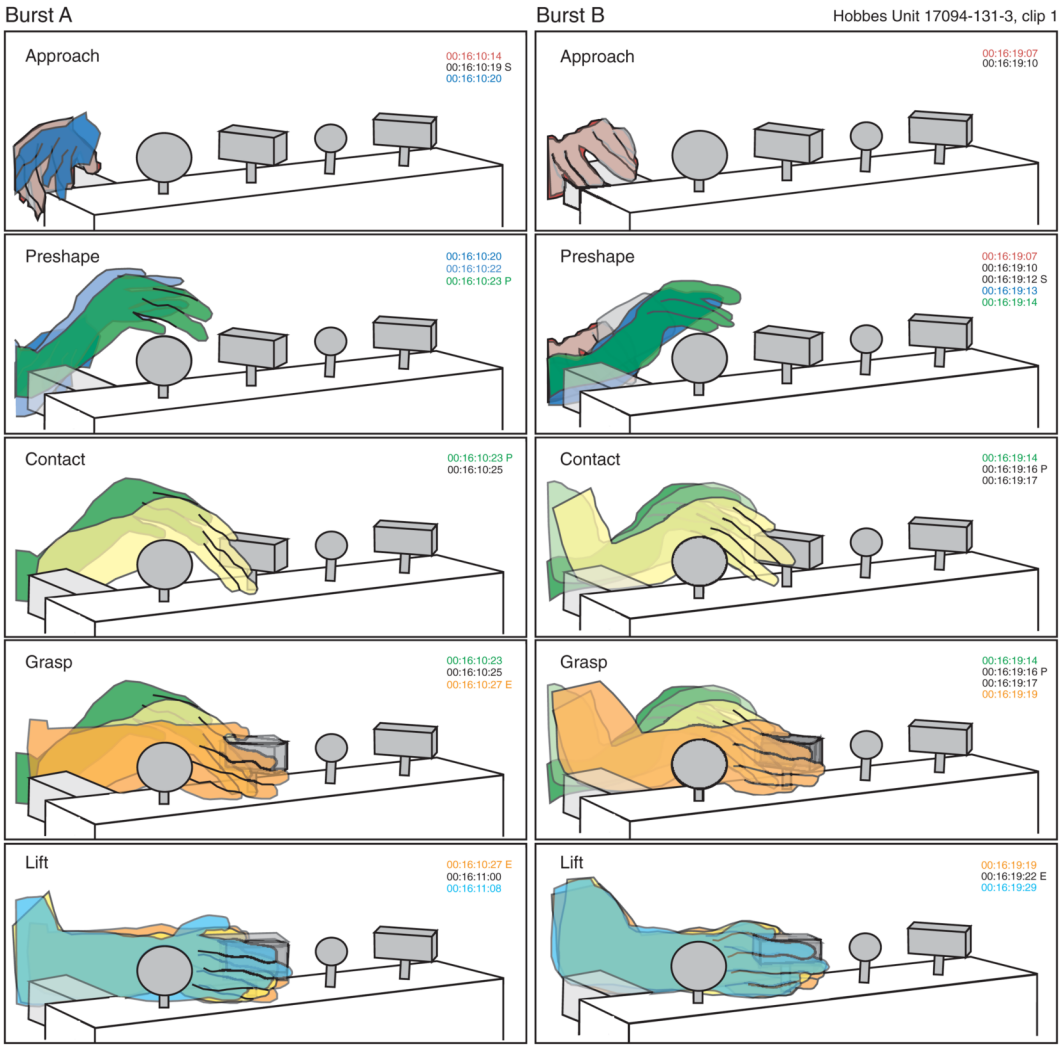

FIG. 4.

Kinematics of forward approach to the rectangular knob. Two trials with the same start and end position are illustrated (*left* and *right*). Note the similarity of reach kinematics and hand placement on the knob. Frames corresponding to the burst start, peak and end are labeled S, P, and E, respectively; maximum firing in these examples occurred as the hand was preshaped during approach.

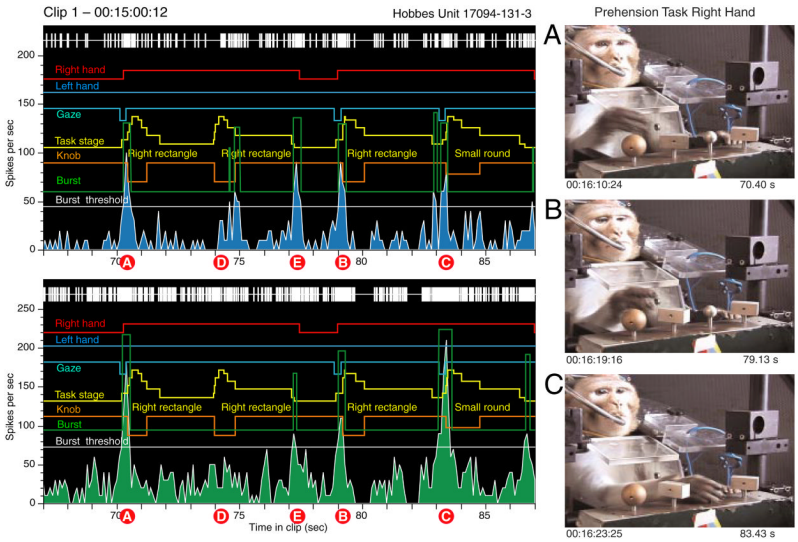

FIG. 5.

Burst analysis of neural responses to the actions shown in Fig. 4. These 2 neurons were recorded simultaneously on 1 electrode in area 5v in the left hemisphere. Task trials and stage onsets are indicated by stepped yellow pyramids; the knob location on the shape box and the duration of hand contact are marked by the orange trace. Other traces illustrate spontaneous actions of the 2 hands (red and blue) and gaze fixation on the target object (cyan, downward deflection). Both neurons reached peak firing rates during the early task stages as the hand approached and contacted the knobs (A–C); regrasps evoked weaker responses (D). The neurons also responded to an aborted reach to the large round knob that ended as he grasped of the chair frame instead (E). Video images to the right were captured at the peaks of bursts A, B, and C.

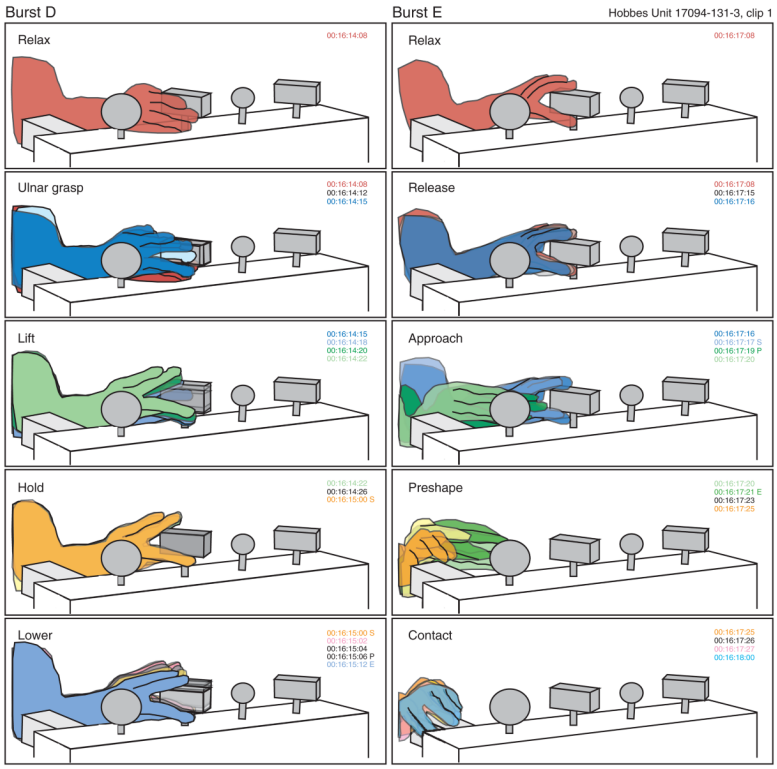

FIG. 6.

Actions performed during bursts D and E of Fig. 5. During burst D, the knob was not fully grasped but lifted instead with the digit tips. Because the hand was left in place on the knob at the end of trial A, there was no reach, and the accompanying neural response was weak. During burst E, the initial actions performed were identical to the start of a lateral approach between knobs, but the animal reached instead to the chair frame where the hand rested until the start of burst B. Neural responses during burst E were similar to task responses during reach.

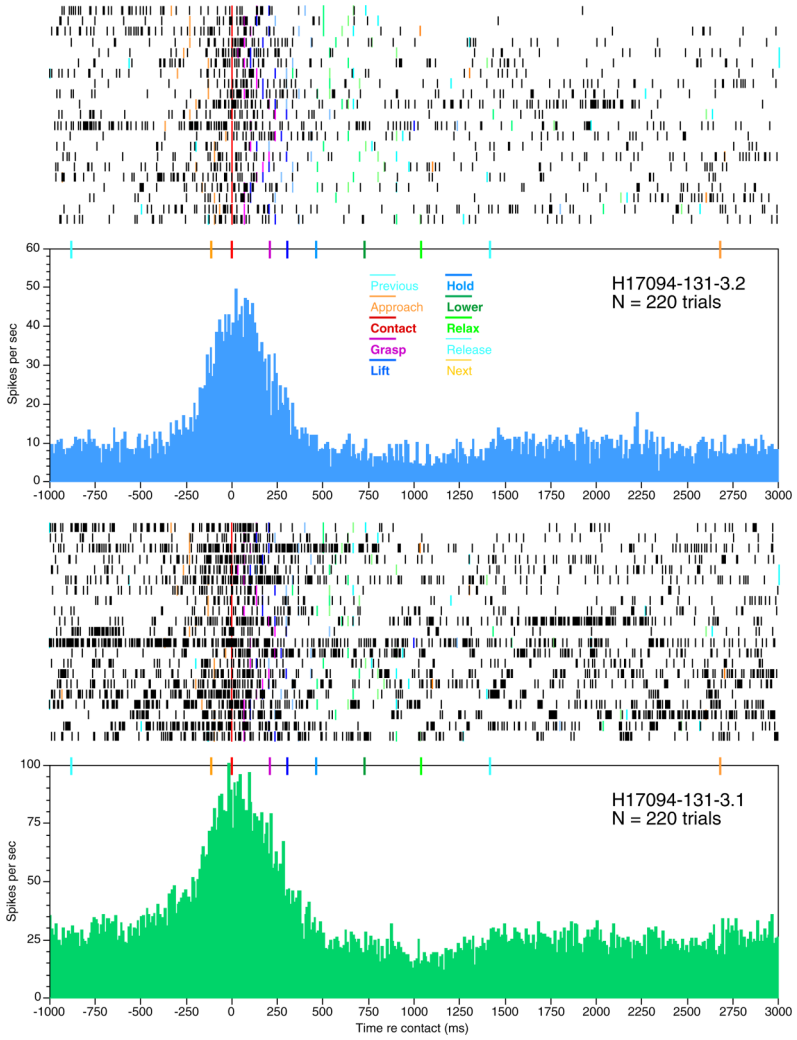

FIG. 7.

Rasters and peristimulus time histograms (PSTHs) aligned to contact with the knob for the neurons shown in Fig. 5. Colored lines on rasters and markers above the PSTH indicate the onset times of task stages relative to contact. PSTHs pool all trials of the four knobs. Only forward and lateral approach trials are shown in the raster. From top to bottom, *trials 1, 7, 10*, and 17 test knob 1 (left rectangle); *trials 2, 3, 6, 11, 16, 18*, and *19* test knob 2 (small round); *trials 4, 5, 8, 13, 15*, and *20* test knob 3 (right rectangle); *trials 2, 9, 12, 14*, and *21* test knob 4 (large round). All 4 knobs evoked similar responses: firing increased at the start of reach, peaked at contact, and declined during lift.

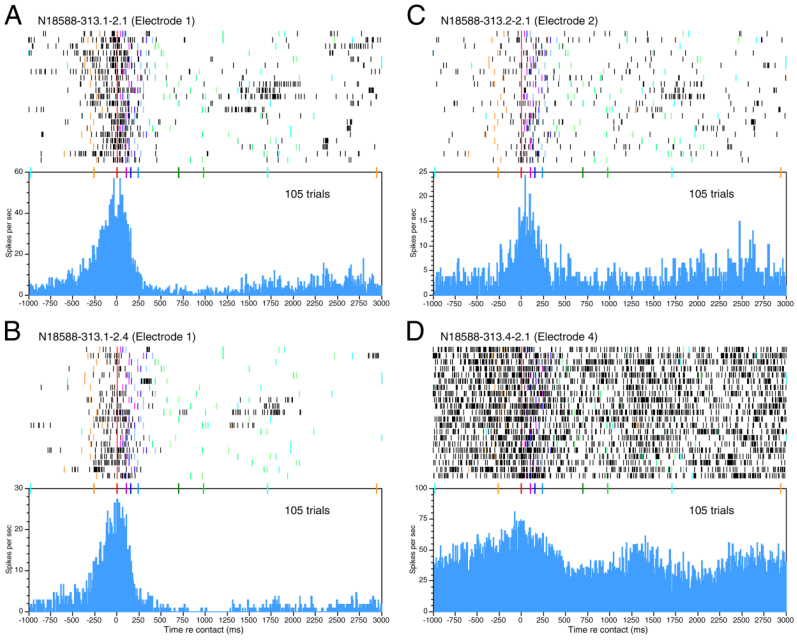

FIG. 8.

Multiple-electrode responses recorded simultaneously from the right hemisphere in *monkey N18588* as he used the left hand. Same format as Fig. 7. Neurons recorded on the same electrode (*A* and *B*) had very similar responses; spike trains recorded on different electrodes (*C* and *D*) had varied responses to identical hand actions. Knob 1 (left rectangle): *trials 1–3, 8 –11*. Knob 2 (large round): *trials 6, 7, 15, 16*. Knob 4 (right rectangle): *trials 4, 5, 12–14, 17–21*. Knob 3 was not cued in the 1st 21 trials.

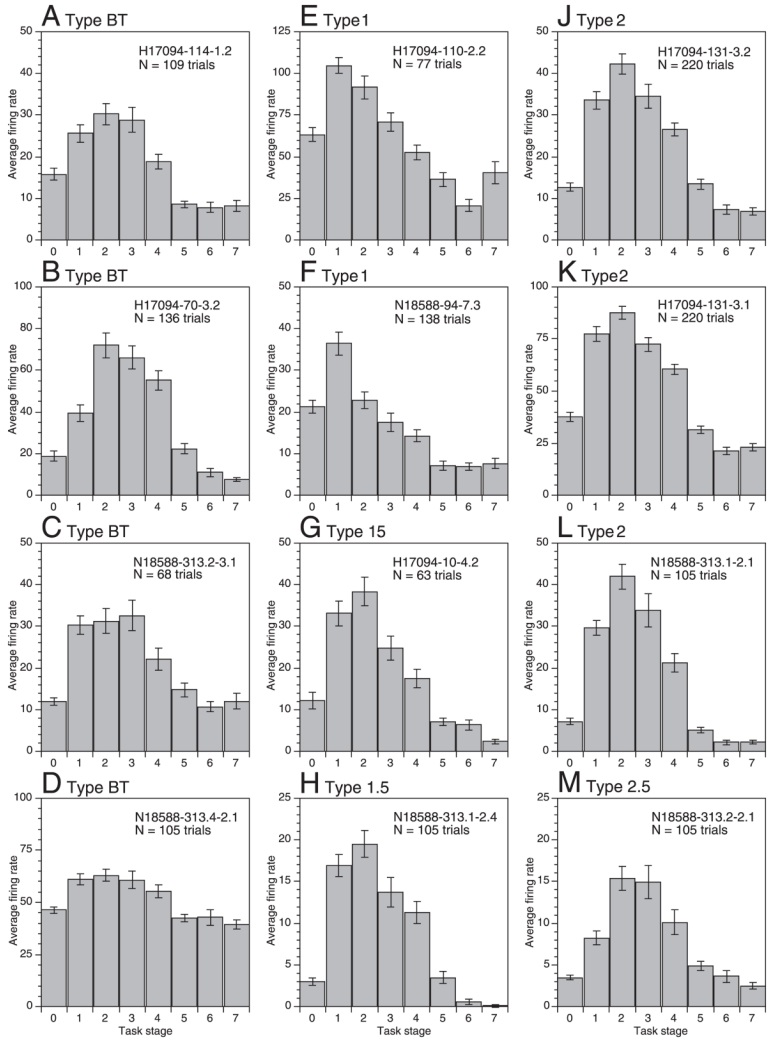

FIG. 9.

Average firing rates per task stage (± SE) for the major response classes in area 5; responses were categorized by the stage(s) in which peak firing occurred. Stage 0 indicates mean firing rate during the pretrial interval. *A–D*: broadly tuned (type BT). *Unit H17094-114-1.2* (*A*), vague response to passive wrist flexion. *Unit H17094-70-3.2* (*B*), flexion of MCP joints and tactile receptive field on dorsum of proximal digit 3. *Units N18588-313.2–3.1* (*C*) and *N18588-313.4–2.1* (*D*), passive receptive fields were not determined. *E* and *F*: approach-tuned (type 1). *Unit H17094-110-2.2* (*E*), receptive field on hairy and glabrous skin of digits, hand, and wrist. *Unit N18588-94-7.3* (*F*), vague tactile receptive field on dorsal hairy skin of forearm, ulnar palm, and digit 5. *G* and *H*: approach-contact (type 1.5). Unit H17094-10-4.2 (*G*), receptive field on the dorsal hairy skin of the hand and digits 2–5. *J–L*: contact-tuned (type 2). *Units H17094-131-3.1* (*J*) and *131–3.2* (*K*), tactile receptive fields located on the glabrous and hairy skin of the hand and digits. *Unit N18588-313.1–2.1* (*L*), passive receptive field was not determined. *M*: contact-grasp (type 2.5). *Unit N18588-313.2–2.1* (*M*), passive receptive field was not determined. Neurons recorded in area 5v are shown in *E* and *F* and *J–K*; the other cells were recorded in area 5d. Average rate graphs for the neurons in Figs. 7 and 8 are shown in *J–K* and *D*, *H*, *L*, and *M*, respectively.

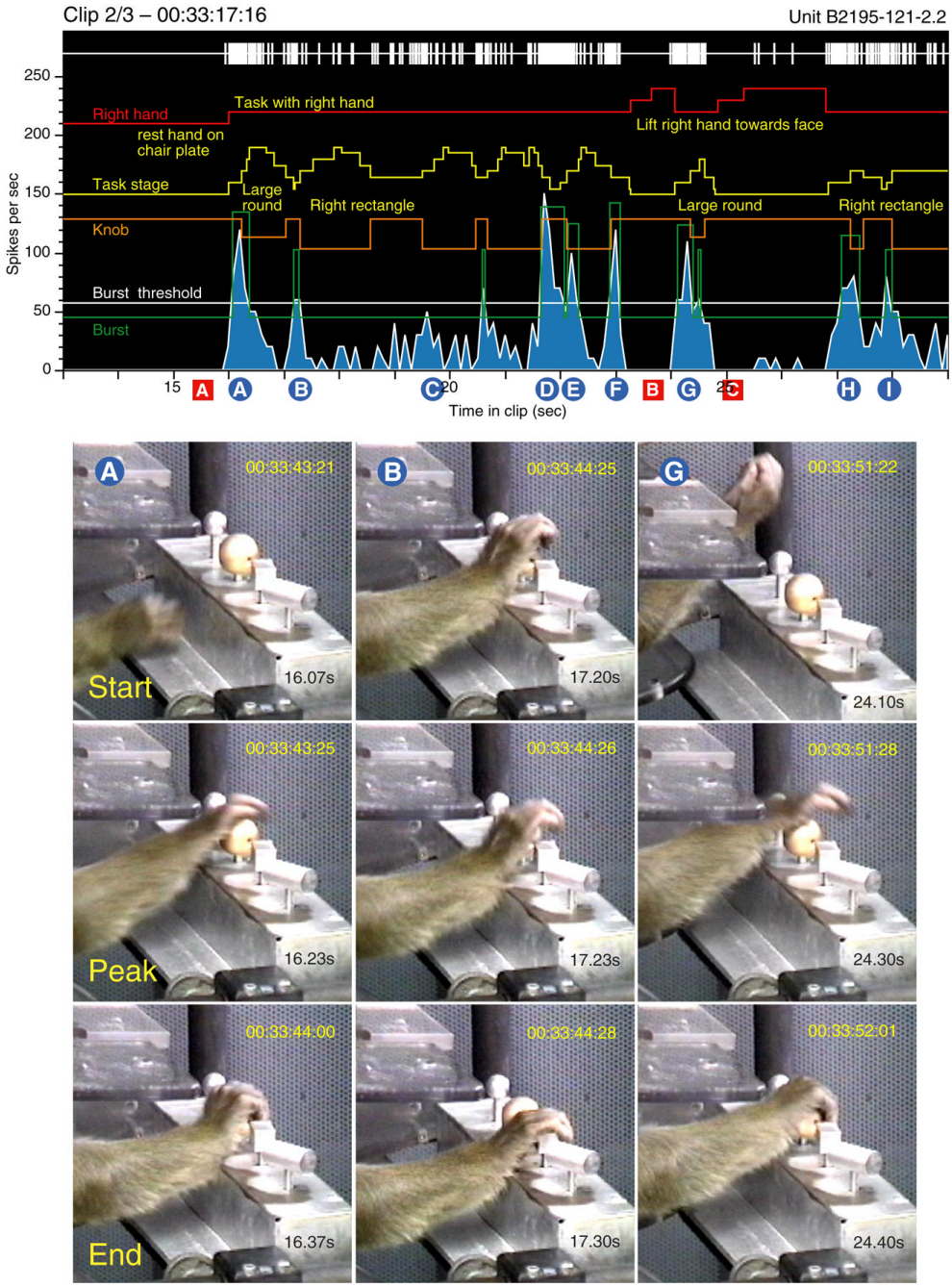

FIG. 10.

Burst analysis illustrating 16 s of continuous recordings from an anterior intraparietal area (AIP) neuron that responded strongly to task-related grasping actions. Video images captured at the start, peak, and end of bursts A, B, and G are shown below the neural records. The burst start coincided with the onset of reach regardless of the point of origin; responses peaked as the hand was pre-shaped over the knob, and ended when the knob was grasped. Task-evoked responses were bracketed by silent epochs when the animal engaged in spontaneous behaviors that failed to excite the neuron; red markers are keyed to examples shown in Fig. 11. The PSTH and average firing rate graph are shown in Fig. 12*B*.

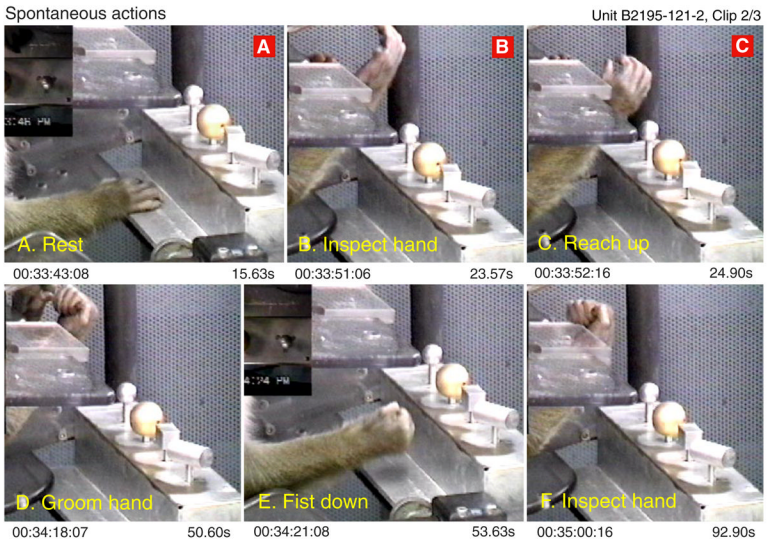

FIG. 11.

Images captured during epochs when the neuron in Fig. 10 fired at low rates or was silent (red A–C); other actions shown were recorded later in this clip. The cell was unresponsive to resting the glabrous hand on a flat surface (*A*) or to flexed hand postures unrelated to object acquisition (*B*, *C*, *D*, and *F*), or to striking the base of the shape box with the fist (*E*).

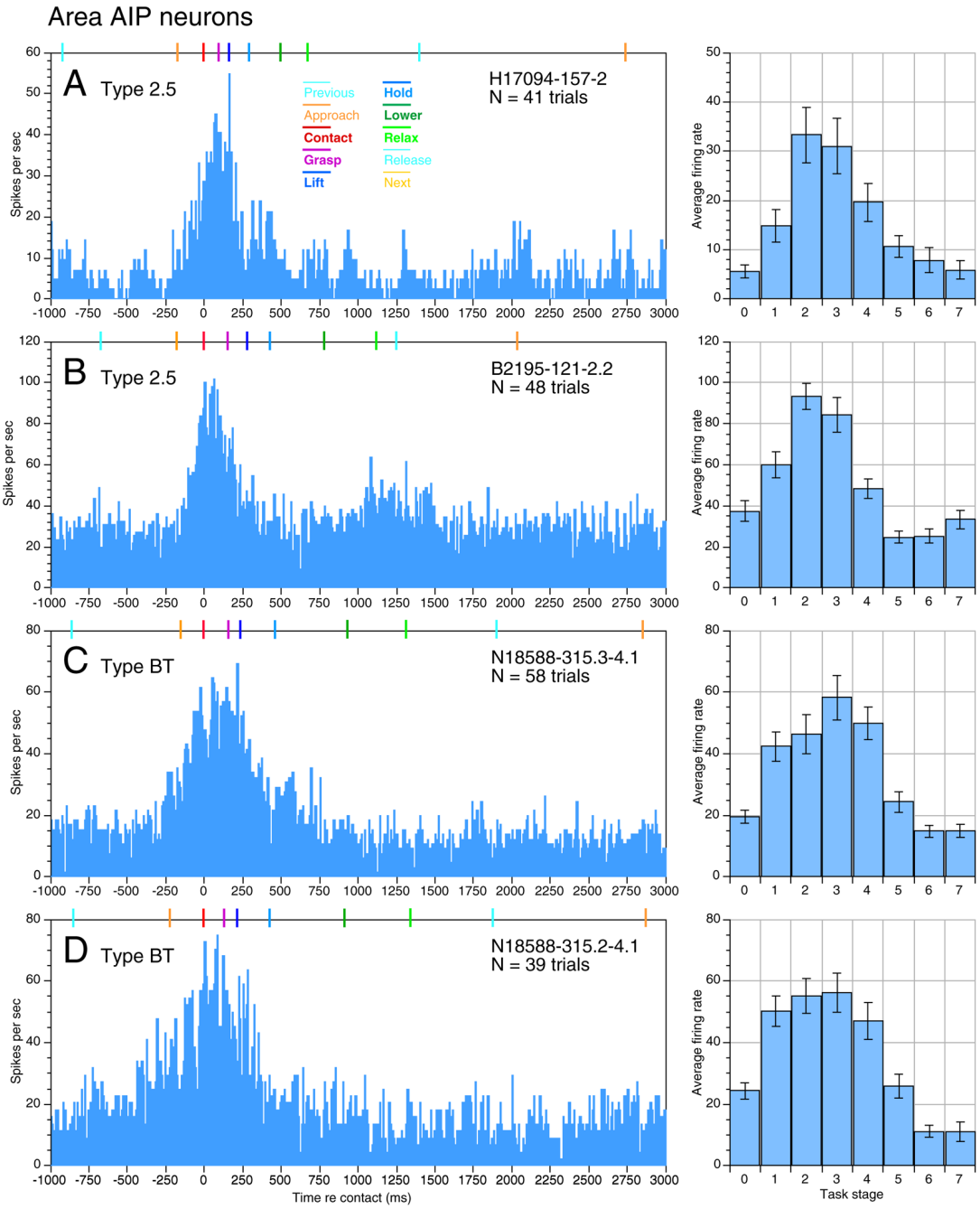

FIG. 12.

PSTHs (*left*) and average firing rate graphs (right) from neurons recorded in area AIP of the 3 animals. Broadly tuned (BT) responses were more common than in area 5. *A: unit H17094-157-2* recorded in the left hemisphere; receptive field not determined. *B: unit B2195-121-2.2*, receptive field located on glabrous skin of digits 2 and 3. Same neuron as in Figs. 11 and 12. *C: unit N18588-315.3– 4.1* recorded on electrode 3 of a multiple electrode array centered in area AIP of the right hemisphere; receptive field not determined. *D: unit N18588-315.2– 4.1* recorded on electrode 2 simultaneously with the neuron shown in *C*.

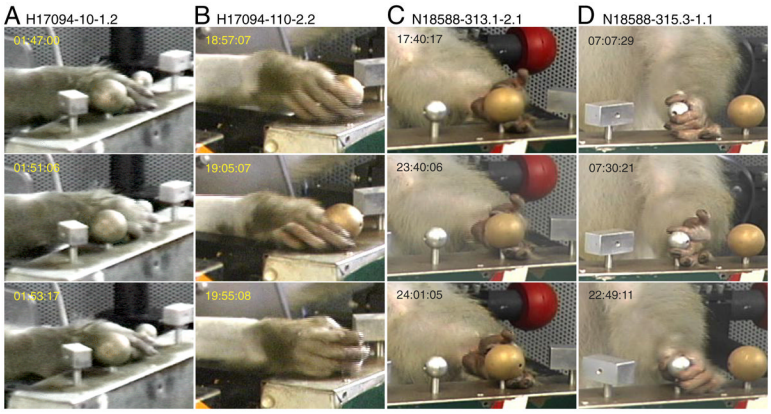

FIG. 13.

Closeup images of the grasp postures used by *monkeys H17094* (*A* and *B*) and *N18588* (*C* and *D*) during trials of the small and large round knobs. Three sequential trials are shown for each knob. Neurons A–C were recorded in area 5, Neuron D in area AIP. Average firing rate graph for Neuron B shown in Fig. 9*E*; rasters and PSTHs for Neuron C are shown in Fig. 8.

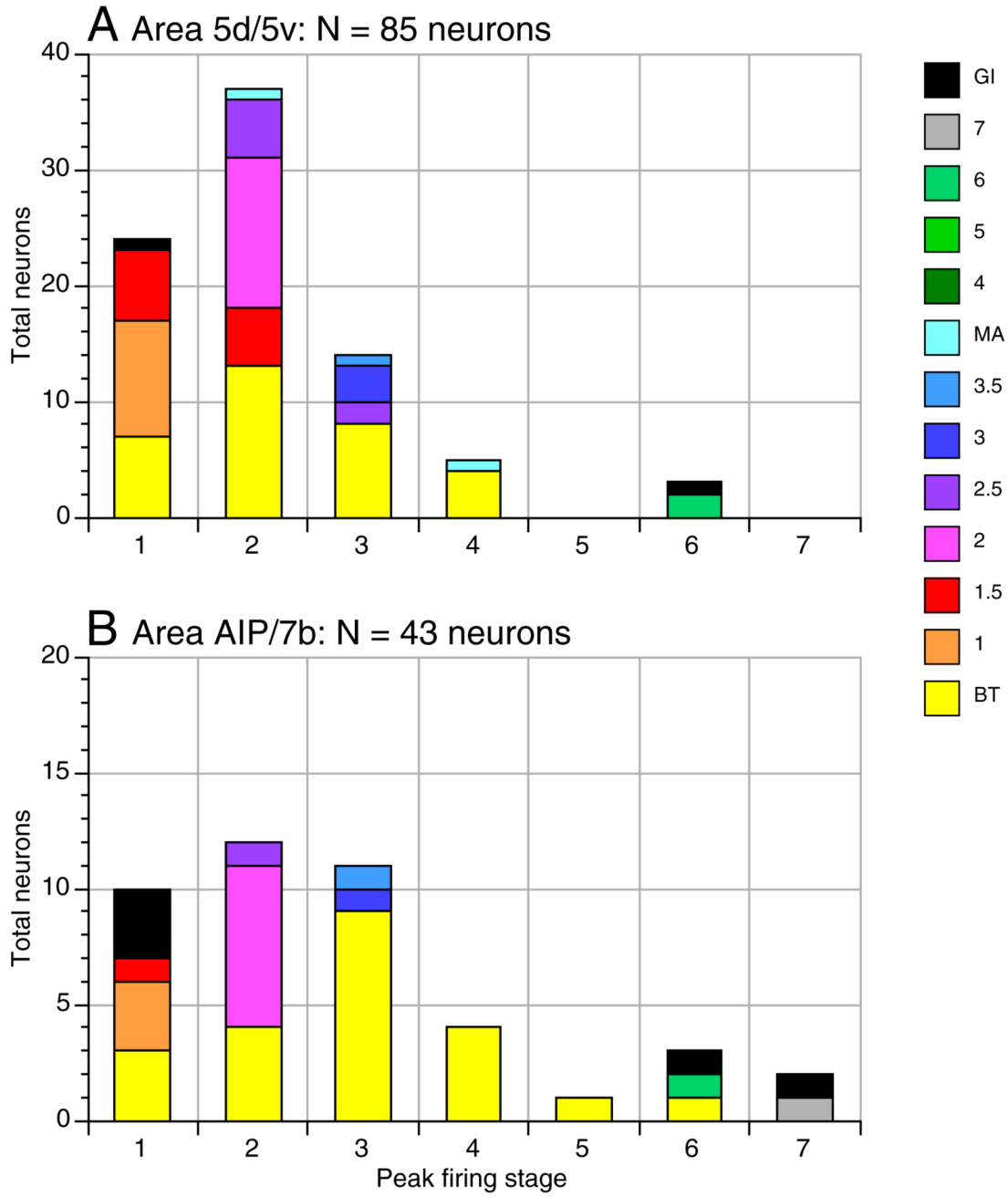

FIG. 14.

Stacked bar graphs of the number and classes of PPC neurons showing peak firing during each task stage. BT, contact-tuned (2), approach-contact (1.5), and approach-tuned (1) were the most common types. Neurons in both SPL and IPL were most likely to fire at peak rates in stage 2 (contact). Approach was the second most common period of peak activity in area 5. Stages 1 and 3 were equally common in area AIP/7b, reflecting the large number of BT neurons recorded there.

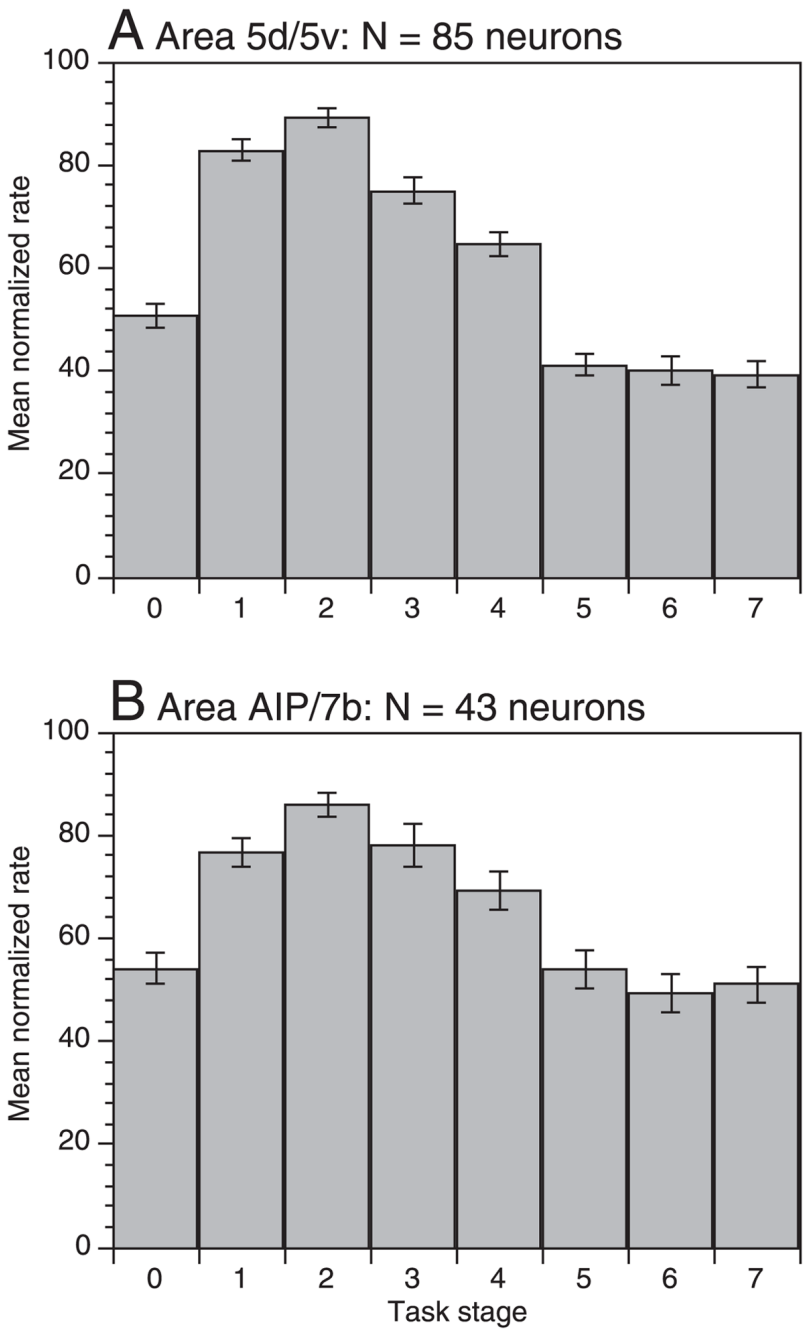

FIG. 15.

Population normalized mean firing rates (± SE) averaged across the entire set of posterior parietal cortex (PPC) neurons tested. Normalized firing rates were computed for each neuron by dividing the mean rate per stage by the maximum value, and multiplying the resultant by 100. Like the peak rates, the mean normalized rate was highest in stage 2 in both areas. Mean firing rates were significantly higher than baseline (stage 0) during stages 1– 4; significant inhibition occurred in stages 5–7 in area 5, and only in stage 6 in area AIP/7b.

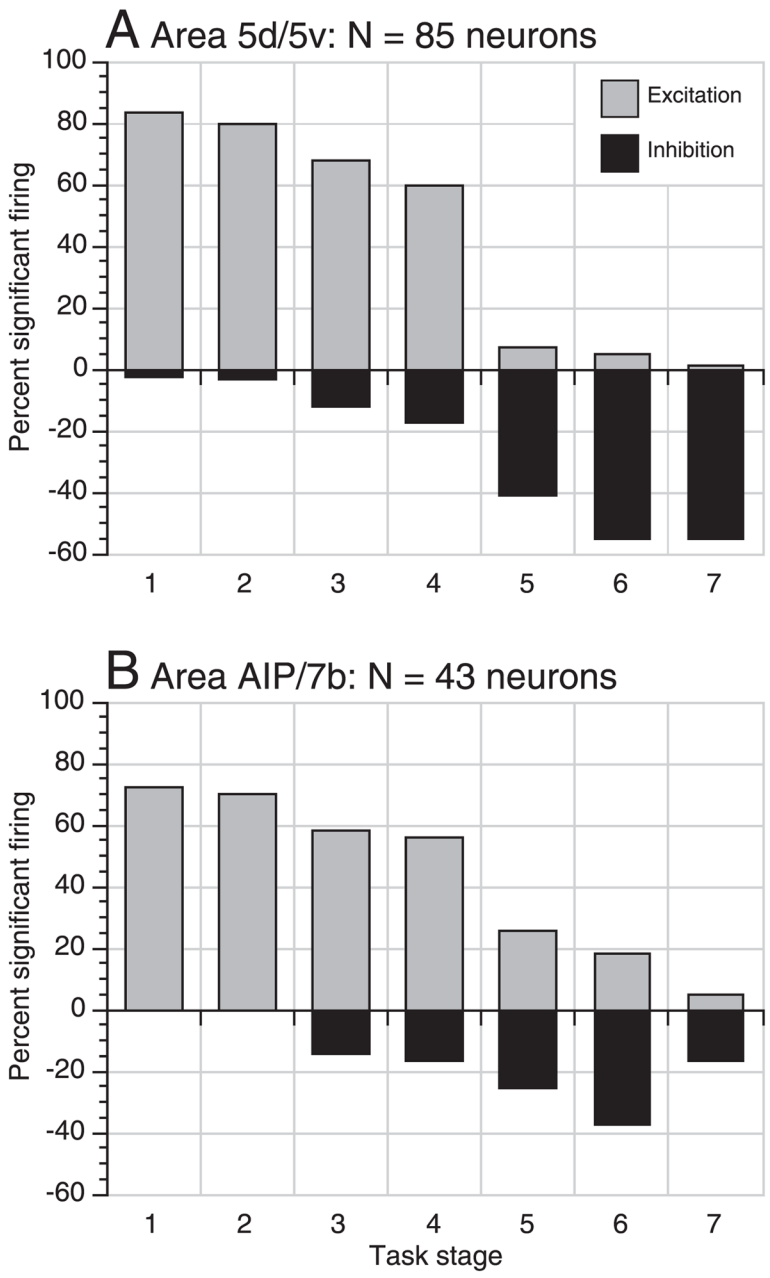

FIG. 16.

Bar graphs showing the percentage of neurons exhibiting significant excitation (gray bars) and inhibition (black bars) during the 7 task stages ($P < 0.05$). Excitation was strongest during stages 1 and 2 and decreased sharply following lift (stage 4); it persisted only in area AIP/7b. during later task stages. Inhibition began in stage 3 (static grasp), and peaked in stage 6 (lower) when the animal prepared to relax the grip.

TABLE 1

Distribution of response classes in PPC

		Area 5D/5V	Area AIP/7b	PPC totals
Response Class	**Label**	**Total Cells**	**Total Cells**	**Total Cells**
Broadly tuned	BT	32 (37.6)	22 (51.2)	54 (42.2)
Approach tuned	1	10 (11.8)	3 (7.0)	13 (10.2)
Approach contact	1.5	11 (12.9)	1 (2.3)	12 (9.4)
Contact tuned	2	13 (15.3)	7 (16.3)	20 (15.6)
Contact grasp	2.5	7 (8.2)	1 (2.3)	8 (6.3)
Grasp tuned	3	3 (3.5)	1 (2.3)	4 (3.1)
Grasp and lift	3.5	1 (1.2)	1 (2.3)	2 (1.6)
Motion activated	MA	2 (2.4)	0 (0.0)	2 (1.6)
Lift tuned	4	0 (0.0)	0 (0.0)	0 (0.0)
Hold tuned	5	0 (0.0)	0 (0.0)	0 (0.0)
Lower tuned	6	2 (2.4)	1 (2.3)	3 (2.3)
Relax tuned	7	0 (0.0)	1 (2.3)	1 (0.8)
Grasp inhibited	GI	4 (4.7)	5 (11.6)	9 (7.0)
Total		85 (100.0)	43 (100.0)	128 (100.0)

Values in parentheses are percentages. PPC, posterior parietal cortex.

TABLE 2

Mean stage duration (ms)

Task Stage	*H17094* (49)		*N18588L* (20)		*N18588R* (50)		*B2195* (88)	
0 Previous	650.3	112.7	542.4	72.0	731.5	27.2	328.1	47.0
1 Approach	131.8	29.9	157.8	30.0	199.9	53.1	140.5	6.4
2 Contact	138.9	39.0	266.8	109.3	127.6	18.6	144.8	39.4
3 Grasp	88.1	29.4	140.8	69.8	50.7	13.7	36.2	6.1
4 Lift	155.9	21.5	199.0	35.5	133.8	48.5	125.4	35.4
5 Hold	385.6	117.0	229.4	67.3	427.7	60.1	222.2	75.6
6 Lower	277.6	65.7	375.3	79.0	301.4	59.7	209.9	62.8
7 Relax	602.6	215.7	379.4	113.2	677.6	84.0	138.4	8.5
Total (1–7)	1780.5	218.7	1746.7	163.1	1918.7	78.3	1017.4	139.5

Mean stage values for all task-related neurons recorded in each animal; values expressed as means ± SD, include neurons recorded in primary somatosensory (S–I) and motor (M–I) cortices as well as in PPC. The shorter duration of stages 0 and 7 in *B2195* reflect the shorter sampling interval per trial in this animal. Number of neurons is in parentheses.